THE UNIVERSITY OF MICHIGAN

COLLEGE OF ENGINEERING
Department of Nuclear Engineering

Final Report

RADIATION EFFECTS STUDIES USING THE MÖSSBAUER EFFECT

D. H. Vincent
J. F. Ullrich

ORA Project 07921

supported by:

NATIONAL SCIENCE FOUNDATION
GRANT NO. GK-871
WASHINGTON, D.C.

administered through:

OFFICE OF RESEARCH ADMINISTRATION ANN ARBOR

June 1969

TABLE OF CONTENTS

I. INTRODUCTION

The NSF Grant GK-871 was extremely important for the initiation of a Mössbauer spectroscopy project within the frame work of the materials research program of the Department of Nuclear Engineering at The University of Michigan. Through it we were able to buy some of the necessary instruments, to support three students during part of their doctoral work, and to cover current costs for materials and supplies for two years. But beyond that the grant was also instrumental in helping us to obtain additional support from other sources: The College of Engineering of The University of Michigan supplied a Nuclear Data 512-channel multichannel analyzer; two grants from the Michigan Memorial Phoenix Project were obtained—one for student support, the other for the acquisition of a liquid helium cryostat; and finally, the Argonne National Laboratory gave financial support to the recipient of this grant in order to make possible his cooperation in that part of the research which was conducted at the Argonne Laboratory.

The original proposal was to study neutron induced recoil defects in tellurium compounds. However, after this investigation was completed to the extent that seemed feasible (see Section II), other problems were attacked. The choice of these was influenced mainly by the general interest that the solution of these problems might have. As will be seen, these investigations did not always fall under the general topic of defect studies by the Mössbauer effect, which we consider as the guiding principle of our research effort.

II. SEARCH FOR RADIATION EFFECTS IN TELLURIUM COMPOUNDS

The principle of our experiments is the following: The source nuclei for the Mössbauer spectroscopy are produced by neutron capture. The energetic gamma rays emitted following neutron capture impart a recoil momentum to the source nucleus. The recoil energy is just large enough to produce a few displacements in the lattice containing the source nucleus. It seems likely, therefore, that the source nucleus itself may end up in a defect position, or that a defect may be located in it's immediate neighborhood. In both cases, the Mössbauer spectrum may be modified in comparison to the undisturbed spectrum either in intensity or in its hyperfine structure, or both. To avoid possible chemical effects it seemed important to require, that the Mössbauer transition should occur in the same nucleus, which is produced by the neutron capture.* This can be achieved in two ways:

1. The Mössbauer transition is observed immediately following neutron capture as the final transition in the capture gamma ray cascade. This makes it necessary to conduct the experiment in the neutron beam at the reactor.

2. The neutron capture process may lead to a long-lived isomeric state. In this case the neutron irradiation of the source may be conducted in the reactor and the isomer produced may be used in a conventional Mössbauer spectrometer away from the reactor.

We have chosen the second possibility.

There are only very few isomers of convenient half-life which may be used for Mössbauer experiments. Out of these we selected Te^{125m} for our experiments.

---

*Usually, Mössbauer sources are β-emitters, i.e. the gamma transition used for resonance absorption occurs in the nucleus which is chemically different from its long-lived radioactive parent.

Our work is described in detail in Appendix A, "Te^{125} Mössbauer Effect Study of Neutron Capture Effects in PbTe, Te and TeO_2."* Our results indicate that the thermal neutron capture process does not affect the Mössbauer spectra of Te^{125} in the compounds investigated. However, we feel that our results, though they are negative in the sense that we did not observe the effect which we had been looking for, have some importance, particularly in view of the fact that Stepanov and Aleksandrov[1] did see an effect in PbTe following neutron irradiation with much higher total doses than ours. Details of the comparison of our measurements with those of the Russian authors are given in Appendix A.

III. MAGNETIC PROPERTIES OF TELLURIUM COMPOUNDS

After the conclusion of the work on defect properties in Te-compounds it was decided to look at the magnetic properties of some Te-compounds. Two facts led to this decision: On one hand we had developed the necessary skill to do Mössbauer spectroscopy with Te^{125} and on the other hand we learned at that time of an interesting ferromagnetic spinel, $CuCr_2Te_4$, which had been the subject of some recent investigations.[2,3,4] This compound seemed to us to offer a unique opportunity to measure transferred hyperfine fields by Mössbauer spectroscopy since Te is the only chalcogenide with a known Mössbauer nuclide and $CuCr_2Te_4$ is the only ferromagnetic spinel which has been successfully prepared using Te as the anion.

A description of the work on $CuCr_2Te_4$ is to be found in Appendix B, which

---

*This paper has been accepted for publication in the Journal of Chemistry and Physics of Solids.

is a reprint of our publication in the Physics Letters.[5] The great interest which this paper aroused may be seen from the fact, that within 6 months of our publication, two other papers appeared in the Physics Letters, one being a measurement of the transferred hyperfine field at the Te^{125}-nucleus in $CuCr_2Te_4$ by NMR techniques,[6] the other being an improvement on our measurement of the magnetic moment of the first excited state in Te^{125}.[7] A recalculation of H_{eff} using the new value for the excited state magnetic moment gives H_{eff} = 164 kgauss; this value is in closer agreement with the NMR results than was our original determination.

Besides $CuCr_2Te_4$, we also remeasured the spectra of two other compounds: antiferromagnetic MnTe and ferromagnetic CrTe. The results of these measurements have not been published and are therefore given here in brief: The MnTe displayed no measurable line broadening, indicating that both the electric quadrupole and magnetic hyperfine interactions are very weak. In conclusion, the antiferromagnetic "superexchange" coupling of the Mn transition metal ions apparently causes little unpairing of the Te spins. Line broadening was observed for CrTe, however it is difficult to ascertain whether the origin is the quadrupole or magnetic interaction. The magnetic interaction is a distinct possibility since the ferromagnetic Cr ions could cause spin unpairing of the Te s-electrons either by exchange polarization or covalent mixing. If the broadening in CrTe is solely magnetic in origin, the internal hyperfine field at the Te site is $H_{eff} \simeq 20$ kgauss.

IV. NEUTRON BEAM EXPERIMENTS WITH Fe^{57} AND K^{40}

Simultaneously with the work described in Section III, we began to look for the Mössbauer effect in Fe^{57} following neutron capture in Fe^{56}. In this case there is no long-lived isomeric state preceding the 14.4 kev transition in Fe^{57} so that the experiment must be conducted in the neutron beam at a reactor. This experiment is quite difficult to do because of the very high gamma background in and around a neutron beam. A carefully designed collimator was built and installed in a beam port at the Ford Nuclear Reactor (FNR) of The University of Michigan. Many arrangements of gamma- and neutron shielding were tested until we were eventually able to see the 14.4 kev radiation as a 4.5% effect above background in a double-window xenon filled proportional counter. At this time we learned that the same experiment had already been done with much higher neutron flux at the FR2-reactor in Karlsruhe, Germany.(8) Since the student engaged in the experiment, a citizen of the Republic of China, faced some problems concerning the extension of his visa, it was then decided, to abandon the experiment at the FNR for the time being and to accept an offer of the Argonne National Laboratory, to conduct similar experiments there. At ANL a number of Mossbauer nuclei were tested in the neutron beam at the CP-5 reactor and K^{40} was eventually chosen as the subject of our investigation. Financial support by the laboratory made it possible for me to actively take part in this investigation during part of the summer 1967, and during shorter trips throughout that year. The results of this work have been published in the Physical Review(9) and may be found as Appendix C to this report.

It is hoped, that Mössbauer experiments in the neutron beam at the FNR

will eventually be taken up again, since recent measurements at Karlsruhe show that this method is one of the most promising for the investigation of radiation effects by Mössbauer spectroscopy.

V. ANALYSIS OF QUADRUPOLE SPLITTING DATA

Guided by the special interest of a graduate student in the Chemistry Department of The University of Michigan, a systematic investigation into the temperature dependence of the quadrupole splitting of some Fe-complex compounds was undertaken. The results of these measurements are appended as Appendix D. Publication of these results with an interpretation of their meaning is intended and reprints of the paper will be submitted when available.

VI. FUTURE PLANS

We are planning to continue our efforts to develop Mossbauer spectroscopy as a tool for the investigation of radiation effects. After a number of unsuccessful attempts in this direction by various authors, Czjzek and Berger have recently obtained very promising results by doing Mössbauer spectroscopy with FeAl-alloys in the neutron beam.[10] Our own work will also concentrate on order-disorder alloys, as well as age-hardening alloys, as will be described in more detail in a new research proposal.

REFERENCES

(1). E. P. Stepanov and A. Yu. Aleksandrov, Change in the Mossbauer Spectrum of Te^{125m} in the Semiconductor PbTe Following Irradiation in a Reactor, ZhETF Pis'ma 5, No. 3, 101-103, 1 February 1967.

(2). F. K. Lotgering, in Proc. Intern. Conf. on Magnetism, Nottingham, England, 1964, 533.

(3). P. K. Baltzer, P. J. Wojtowicz, M. Robbins, and E. Lopatin, Phys. Rev. 151, 367 (1966).

(4). C. Colominas, Phys. Rev. 153, 558 (1967).

(5). J. F. Ullrich and D. H. Vincent, Phys. Letters 25A, 731 (1967).

(6). S. B. Berger, J. I. Budnick, and T. J. Burch, Phys. Letters 26A, 450 (1968).

(7). R. B. Frankel, J. J. Huntzicker, D. A. Shirley, and N. J. Stone, Phys. Letters 26A, 452 (1968).

(8). W. G. Berger, J. Fink, and F. E. Obenshain, Phys. Letters 25A, 466 (1967).

(9). P. K. Tseng, S. L. Ruby, and D. H. Vincent, Phys. Rev. 172, 249 (1968).

(10). W. G. Berger and Gordon Czjzek, private communication (1968).

APPENDIX A

"Te^{125} Mössbauer Effect Study of Neutron Capture Effects in PbTe, Te, and TeO_2"

by

J. F. Ullrich and D. H. Vincent

Accepted for publication in the Journal of Physics and Chemistry of Solids

J. Phys. Chem. Solids Pergamon Press 1969. Vol. 30, pp. 1189–1195. Printed in Great Britain.

Te^{125} MÖSSBAUER EFFECT STUDY OF NEUTRON CAPTURE EFFECTS IN PbTe, Te AND TeO_2*

J. F. ULLRICH† and D. H. VINCENT
Department of Nuclear Engineering, University of Michigan, Ann Arbor, Mich. 48104, U.S.A.

(*Received* 28 *August* 1968; *in revised form* 4 *November* 1968)

Abstract – The Mössbauer emission spectra of Te^{125} in PbTe, Te metal, and TeO_2 have been measured following neutron capture in Te^{124}. Mössbauer data for each sample were taken after the source irradiation and following thermal annealing. The irradiation conditions were chosen so that only the thermal neutron capture induced defects should have a significant effect on the environment of the Mössbauer emitting nuclei. Comparison of the data taken before and after the source annealing showed no differences in linewidth, isomer shift, quadrupole splitting, or resonance intensity within the standard deviations of the parameters. The results show that the thermal neutron capture process in Te^{124} does not affect the Te^{125} Mössbauer spectra. The possible reasons for this are discussed. The results also indicate that the anomalous isomer shift reported by Stepanov and Aleksandrov in a similar experiment on PbTe is probably caused by a high background of fast neutron induced displacements.

1. INTRODUCTION

CHANGES in the structure of Mössbauer emission spectra due to the presence of neutron capture induced displacements have been studied in processes involving both neutron activation of the first excited state of the Mössbauer nuclide[1–3] and neutron activation of an isomeric state parent[4, 5]. Because of the short lifetime of the first excited state of Mössbauer nuclides (10^{-10}–10^{-5} sec), the neutron activation of this state and the Mössbauer measurement must be done simultaneously. Thus, the first type of experiment must be done in a neutron beam. However, if the Mössbauer nuclide has a long-lived isomeric state, then the neutron activation and the Mössbauer measurement can be done at different times. In the second type of experiment the neutron irradiation can be done in-pile and the Mössbauer measurement can be made at leisure after the irradiation.

The principle advantage of the second type of experiment is that it avoids the usual problems of low neutron intensity and high background radiation associated with neutron beam experiments. There is one limitation, however, in the use of in-pile irradiations for investigating radiation effects; the measurements are restricted to materials with defect annealing temperatures greater than the reactor irradiation temperature (generally 50°C or higher). This severely limits the number of potential experiments. This, of course, is not true if low temperature irradiations are possible; however, low temperature irradiation facilities are not available at most reactors.

Sn^{119} and Te^{125} are two Mössbauer nuclides that offer favorable thermal neutron capture cross sections, isomeric state half-lives, and resonant gamma ray energies for use in the second type of experiment. Previous Mössbauer investigations of the effect of neutron irradiation on the resonant emission spectra of these nuclides have given some evidence of recoil induced changes in the electronic configuration about the emitting nuclei.

Hannaford *et al.*[4] found a small satellite peak in the emission spectrum of Sn^{119} in Mg_2SnO_4 following neutron activation. The

*Research supported by the National Science Foundation, Grant No. Gk-871.

†*Present address*: Scientific Laboratory, Ford Motor Company, Dearborn, Michigan.

intensity and isomer shift of the satellite peak indicated that approximately 25 per cent of the Sn atoms had suffered a recoil induced valency change. The valency change was clearly shown to be attributable to neutron capture induced displacements.

Stepanov and Aleksandrov[5] recently reported a Mössbauer measurement on Te^{125} in PbTe following neutron activation. The measurement showed an anomalous isomer shift. The PbTe source measured against a PbTe absorber had an isomer shift of 1·7 mm/sec (measured 20 days after the end of the irradiation) when, in fact, there should be no isomer shift if the source and absorber are chemically identical. The anomalous isomer shift indicated that the *s*-electron configuration of the PbTe source had been altered by the irradiation. The anomalous isomer shift was observed to decrease exponentially with time with a mean life of 10 ± 3 days. This indicated that the defect structure was annealed at room temperature.

The measurements reported in this paper were also done on Te^{125} following neutron activation. In addition to a measurement on PbTe, measurements were also made on Te metal and TeO_2. Mössbauer measurements were made on each of the three materials following the source irradiation and then following thermal annealing of the same source. The two spectra were then compared to see if there were any changes in the hyperfine spectra caused by neutron capture induced displacements.

Contrary to the results of Stepanov and Aleksandrov the Mössbauer spectrum for PbTe reported in this paper showed no anomalous isomer shift after the neutron irradiation. In fact, no changes were observed in the hyperfine spectra of any of the three materials.

The difference between these results for PbTe and those of Stepanov and Aleksandrov yields considerable insight into the defect mechanisms involved. The measurements reported in this paper were made with irradiation conditions chosen so that the Mössbauer spectra should only be affected by displacements caused by the thermal neutron capture process. The results indicate that the thermal neutron capture process in Te^{124} does not have an effect on the Mössbauer spectra of the Te^{125}. In conclusion, the anomaly observed by Stepanov and Aleksandrov in PbTe is probably the result of a high concentration of displacements induced by mechanisms other than thermal neutron capture. The most likely mechanism is fast neutron elastic scattering.

2. RADIATION EFFECTS

The Mössbauer isomeric state parent $Te^{125m}(58d)$ is produced by thermal neutron capture in Te^{124} (i.e. $Te^{124} + n_{th} \rightarrow Te^{125m} + \gamma$). The Te^{125m} nucleus can be introduced into the lattice as a defect if the recoil energy from the (n, γ)-reaction is greater than the minimum energy for displacement, E_d, which is typically of the order of 25 eV. The recoil energy arises from the emission of the 6·4 MeV of excitation energy of Te^{125} by 'prompt' gamma rays. By conservation of momentum the emitted gamma rays impart kinetic energy to the emitting nucleus.

A calculation of the mean recoil energy requires knowledge of the gamma rays emitted in the de-excitation process, including their energies, emission probabilities, and time and angular correlation. Unfortunatley the capture gamma ray energy spectrum has not been measured for neutron capture in Te^{124}; therefore the mean recoil energy cannot be accurately estimated.

In general the mean recoil energy for capture gamma ray emission is low (of the order of E_d). This means that the number of displaced atoms produced per thermal neutron captured is small; subsequently, the number of possible defect configuration is small. This is a particularly nice feature for Mössbauer measurements since the resultant Mössbauer spectrum is a weighted sum of the spectra characteristic of each defect configuration.

The isolation of displacements which are induced specifically by thermal neutrons is often very difficult when doing in-pile irradiations. This is due to the 'background' effects caused by displacements due to other recoil processes. All of the types of radiation present in a reactor (i.e. fast neutrons, gamma rays, etc.) can produce displacements through either scattering processes or nuclear reactions. For most elements the ratio of defects produced by thermal neutron capture to those produced by fast neutron scattering is less than one[6]. Thus, fast neutrons are usually responsible for most of the radiation effects observed with in-pile irradiations.

Under some conditions the Mössbauer effect measurement provides a means of separating displacements due to thermal neutron capture from those arising from fast neutrons and other sources. This is possible because the characteristic hyperfine interactions are, for the most part, only influenced by the 'local' electronic environment (atomic electrons and first few near neighbour atoms).

The fraction of the resonant emissions which have hyperfine structure characteristic of a defect environment is related to the probability that a defect is within the 'local' environment of an emitting nucleus. For defects produced by thermal neutron capture this probability should be nearly equal to 1 since the emitting nucleus itself is in a defect position. On the other hand, defects produced by other types of radiation are randomly located with respect to the emitting nuclei. Hence the probability that these defects are within the 'local' environment of an emitting nucleus is of the order of the ratio of the defect density to the appropriate atomic density.*

In order to minimize the effect of displacements caused by other types of radiation, the density of defects must be kept much less than the number density of atoms. Since the defect density is a linear function of the total radiation dose (in the absence of self annealing), it is possible to minimize the effect of undesirable displacements by proper choice of irradiation fluxes and times.

The measurements reported in this paper were carried out under conditions where the thermal neutron capture effects played a dominant role. Fast neutron scattering was the principal source of additional displacements; however, the estimated density of these displacements was $\sim 10^{-4}$–10^{-3} of the tellurium atom density. Thus, the fraction of Mössbauer emitting nuclei which are in close proximity to a fast neutron displaced atom is very small. The fast neutron induced displacements then should have little effect on the Mössbauer spectra.

3. EXPERIMENTAL PROCEDURE

(*A*) *Sources and absorbers*

The PbTe, Te metal and TeO_2 used in the measurements as sources were prepared from Te enriched to 94 per cent in Te^{124}. The PbTe† and Te metal powders were pressed into thin discs and then sintered in a hydrogen atmosphere at 550°C for 3 hr and 350°C for 6 hr, respectively. The TeO_2 was prepared from nitric acid solution following the procedure of Marshall[7]. This procedure results in TeO_2 with the tetragonal crystal structure. The structures of the materials were all verified by X-ray diffraction measurement.

The materials to be used as sources were irradiated in the Ford Nuclear Reactor. Samples were generally irradiated in fluxes of 10^{12}–10^{13} neutrons/cm^2-sec for periods of 10–15 days. The total thermal neutron doses for the PbTe, Te and TeO_2 samples reported on in this paper were 8×10^{17}, 9×10^{17} and 8×10^{18} neutron/cm^2, respectively. The fast neutron doses were a factor of 12 lower.

*The atomic density used here must take into account the range of the hyperfine interactions (referred to as the 'local' environment). This density will be smaller than the number density of atoms for long range interactions and will approach the number density for short range interactions (hyperfine interactions affected only by the atomic electrons).

†Prepared by New England Nuclear Corp., Boston, Mass.

The sample temperatures during the irradiation were measured to be ~45°C.

After the Mössbauer measurement was made following the source irradiation, the sources were all annealed to restore any displaced atoms to normal lattice sites. The PbTe and Te sources were annealed in a hydrogen atmosphere at 400°C for 11 hr and 350°C for 12 hr, respectively. The TeO_2 was dissolved in HNO_3 and recrystallized following the procedure in the initial preparation.

The Mössbauer measurements for PbTe and Te were made using a single line absorber of PbTe (17·5 mg/cm²) enriched to 95 per cent in Te^{125}. The measurements for TeO_2 were made using a single line absorber of $Te(OH)_6$ (39 mg/cm²) with a natural abundance of Te^{125} (7 per cent).

(B) Apparatus

The Mössbauer measurements were made using the 35·6 keV gamma ray resonance in Te^{125}. Details of the decay scheme and the relevant Mössbauer parameters have previously been reported [8].

The 35·6 keV gamma rays were detected using a xenon–nitrogen filled proportional counter. With this detector the 35·6 keV gamma ray is only partially resolved from the intense background due to the Te K_α and K_β X-rays at 27·4 and 31·2 keV. The gamma ray can best be discriminated by using the escape peak at 7·0 keV. All measurements were made with the single channel analyzer set at the escape peak energy.

The signal-to-noise ratio of the escape peak was further improved by using a 5 mil copper (113 mg/cm²) absorber to reduce the X-ray intensity. This increased the signal-to-noise ratio by a factor of 3·5 with only a factor of 0·33 reduction in the count rate. The 8·0 keV copper X-rays which are generated in this absorber are almost completely absorbed in the 20 mil aluminum window on the proportional counter.

The resonant absorption spectra were taken using a time mode Mössbauer spectrometer. The multichannel analyzer was calibrated using the magnetic hyperfine spectrum of Fe^{57} in iron metal. Calibration runs were made before and after each Te run to check the constancy of the equipment.

The source and absorber were both cooled to liquid nitrogen temperature in a styrofoam insulated dewar similar to the one described by DeWaard *et al.*[9]. The source and absorber temperatures were not externally controlled and were generally ~ 82°K.

4. RESULTS

The results of the measurements on PbTe, Te and TeO_2 are shown in Fig. 1. The data points shown are those taken in the Mössbauer measurements immediately following the

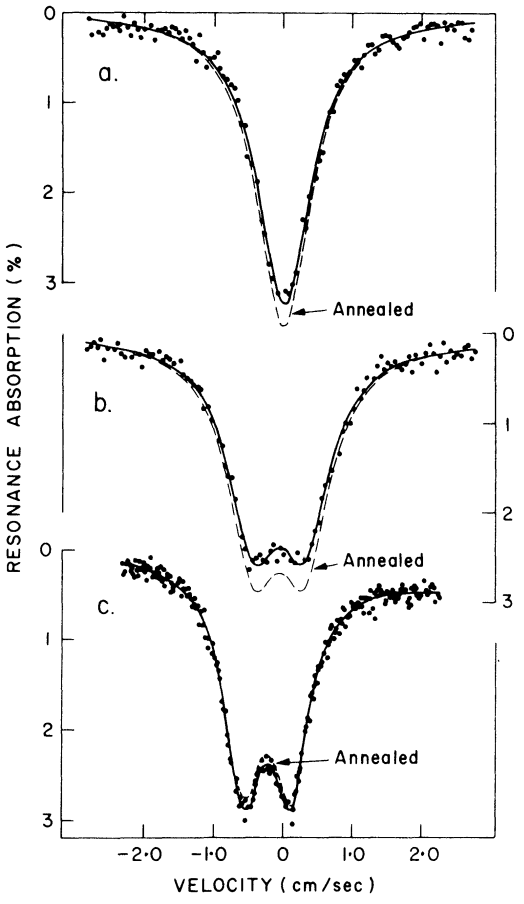

Fig. 1. Resonance absorption spectra taken before and after source annealing for: (a) PbTe; (b) Te metal; (c) TeO_2.

irradiations. The solid line is the least squares fit to the data with an assumed spectral shape. A single line of Lorentzian shape was fit to the PbTe spectrum and two lines of Lorentzian shape (quadrupole split) were fit to the Te and TeO_2 spectra.

The spectra characteristic of the normal lattices were obtained after treating the sources to restore any displaced atoms to normal lattice sites. The results of the curve fitting to the Mössbauer spectra taken after annealing are shown in Fig. 1. by the dashed lines.

The parameters obtained from the least squares fit to the spectra taken before and after annealing are listed in Table 1. The standard deviations of the parameters listed in the table are calculated from the error matrix generated in the final iteration of the least squares fitting routine. It is apparent from this tabulation that the linewidth, the isomer shift and the quadrupole splitting for the three materials are identical in the two runs within the standard deviations of the parameters.

Table 1. *Parameters obtained from the least squares fit to the data of Fig.* 1

Source		Linewidth (mm/sec)	Isomer shift* (mm/sec)	Quadrupole splitting (mm/sec)	Resonance intensity†
PbTe	– Pre-anneal	9·69 ± 0·23	0·07 ± 0·05	0	0·0324 ± 0·0003
	Post-anneal	9·58 ± 0·22	0·03 ± 0·04	0	0·0351 ± 0·0003
Te	– Pre-anneal	9·07 ± 0·24	−0·44 ± 0·08	7·51 ± 0·14	0·0197 ± 0·0004
	Post-anneal	8·83 ± 0·26	−0·41 ± 0·09	7·35 ± 0·15	0·0221 ± 0·0005
TeO_2	– Pre-anneal	6·42 ± 0·12	−1·98 ± 0·04	6·72 ± 0·11	0·0226 ± 0·0002
	Post-anneal	6·49 ± 0·12	−1·99 ± 0·04	6·89 ± 0·11	0·0219 ± 0·0002

*Shift relative to PbTe for the PbTe and Te source and $Te(OH)_6$ for the TeO_2 source.
†Maximum resonance intensity uncorrected for background.

The only parameter which shows a significant variation between runs is the resonance intensity. In all cases the variation in resonance intensity (3–11 per cent) is greater than the standard deviation in the intensity parameter (1–2 per cent). However, this standard deviation reflects only the statistical uncertainty in the fitting and does not include a contribution due to variations in experimental conditions. Several experimental factors can have a significant effect on the measured resonance intensity. These include the detector signal-to-noise ratio, the source and absorber temperature, and the experimental geometry. An accurate comparison of resonance intensities for two different runs requires that these factors not only remain stable during the course of each run but be exactly reproducible for each run. In both respects the conditions for our experiments were not the most desirable. Runs were generally of the order of 4–5 days in duration; this, of course, put a limitation on the temperature and electronic stability. In addition, the samples had to be removed between runs for annealing; this made exact reproducibility of all conditions difficult. A careful analysis of the stability and reproducibility of all the previously mentioned factors for our measurements indicates that the experimental uncertainty in the resonance intensity amounts to about 10 per cent.

As a result, the observed variations in the resonance intensity are only of the order of the uncertainty in the measured intensity. To see if the variations in resonance intensity for each material were reproducible, the sets of measurements were repeated using new sources. This second set of measurements for each material (only the measurements with the best statistics are reported in this paper)

did not show the same variation in resonance intensity as the first set. In all cases the magnitude of the change was different and in one case even the direction of the change was different. Again, as in the first set of measurements, the resonance intensity changes ranged up to about 10 per cent.

From this evidence we conclude that if there are any f value changes in any of the materials due to the source irradiation, the change is certainly less than 10 per cent of the normal f value. To determine whether or not there indeed is a real f value change would require that the experimental conditions be much better controlled than in our measurements.

The quadrupole splittings for Te and TeO_2 obtained in our measurements are in agreement with previously reported values. All previous results, except for a recent measurement by Pasternak and Bukshpan[10], are summarized in a paper by Violet and Booth [11]. For comparison with previous results, the values obtained for the quadrupole splitting in our measurements are $0{\cdot}75 \pm 0{\cdot}01$ cm/sec and $0{\cdot}69 \pm 0{\cdot}01$ cm/sec* for Te metal and TeO_2, respectively.

To compare isomer shifts with the values tabulated by Violet and Booth, our values have all been referred to a Te source. With respect to a Te source, the isomer shifts are $-0{\cdot}04 \pm 0{\cdot}01$ cm/sec and $+0{\cdot}02 \pm 0{\cdot}01$ cm/sec for PbTe and TeO_2†, respectively. The isomer shift for TeO_2 agrees with the value obtained by Violet and Booth; however the isomer shift for PbTe is less than the value reported by Stepanov *et al.*[12].

5. DISCUSSION

Our measurements show no clearly resolved changes in the Mössbauer hyperfine spectra of Te^{125} which could be attributed to neutron capture induced recoils. There are several possible explanations for the lack of any observable effects; however, it is difficult to establish any conclusive explanation due to the lack of supplemental information.

First, the changes in the hyperfine structure may be too small to be resolved. The broad lines of the Te^{125} resonance, of course, make observation of small changes in the hyperfine spectra very difficult. It is also very difficult to theoretically predict the isomer shift and electric quadrupole splitting that might occur for various possible defect configurations.

Second, there may be insufficient recoil energy on the average to displace the atoms from their normal lattice sites.

Third, defect annealing may occur at the reactor irradiation temperature of 45°C. Previous measurements indicate that such annealing probably does occur in Te metal, but definitely not in PbTe. A study of electron bombardment effects on Te metal showed that the defects anneal fairly rapidly even at room temperature[13]. Rather extensive measurements of the Hall coefficient, the Seebeck coefficient, the electrical resistivity and the thermal conductivity of PbTe both during and following thermal and fast neutron irradiation show little annealing below temperatures $\sim$ 150°C[14, 15]. There are no previous measurements of radiation effects in TeO_2.

It is quite clear from our results that the thermal neutron capture process in Te^{124} does not lead to any significant changes in the Mössbauer hyperfine spectra. The PbTe data, in particular, give evidence that the isomer shift anomaly observed by Stepanov and Aleksandrov is probably caused by displacements induced by other types of reactor radiation. All the measurements reported in this paper were made within approximately three weeks after the end of the irradiation. Using Stepanov and Aleksandrov's annealing curve, an isomer shift of at least 1·5 mm/sec should have been observed if the anomaly was

*The values quoted here are the average values obtained from several runs.

†The TeO_2 isomer shift was obtained by combining the results reported in this paper with an additional measurement with a PbTe source and Te(OH)6 absorber which showed an isomer shift of $-0{\cdot}13 \pm 0{\cdot}01$ cm/sec.

caused by neutron capture induced recoils.

The most likely cause of the isomer shift anomaly observed by Stepanov and Aleksandrov is fast neutron induced displacements. No information is given on the fast neutron flux used in their irradiation; however, if it is assumed that the fast flux is $\frac{1}{10}$ the magnitude of the thermal flux quoted in their paper and that there is no saturation of defects, the Te defect density could be as large as $\frac{1}{5}$ the Te atomic density. Thus the Stepanov and Aleksandrov measurement seems to have been carried out under irradiation conditions where 'background' displacements have a high enough density to significantly affect the Mössbauer spectrum.

REFERENCES

1. HAFEMEISTER D. W. and SHERA E. B., *Phys. Rev. Lett.* **14**, 593 (1965).
2. FINK J. and KIENLE P., *Phys. Lett.* **17**, 326 (1965).
3. BERGER W. G., FINK J. and OBENSHAIN F. E., *Phys. Lett.* **25A**, 466 (1967).
4. HANNAFORD F., HOWARD C. J. and WIGNALL J. W. G., *Phys. Lett.* **19**, 257 (1965).
5. STEPANOV E. P. and ALEKSANDROV A. YU., *JETP Lett.* **5**, 83 (1967).
6. WALKER R. M., *J. nucl. Mater.* **2**, 147 (1960).
7. MARSHALL H., In *Inorganic Syntheses* (Edited by L. F. Audrieth), Vol. 3. McGraw-Hill, New York (1950).
8. See *Mössbauer Effect Data Index* (Compiled by A. H. Muir Jr., K. J. Ando and H. M. Coogan). Interscience, New York (1966).
9. DeWAARD H., DEPASQUALI G. and HAFEMEISTER D., *Phys. Lett.* **5**, 217 (1963).
10. PASTERNAK M. and BUKSHPAN S., *Phys. Rev.* **163**, 297 (1967).
11. VIOLET C. E. and BOOTH R., *Phys. Rev.* **144**, 225 (1966).
12. STEPANOV E. P., ALESHIN K. P., MANAPOV R. A., SAMOILOV B. N., SKLYAREVSKY V. V. and STANKEVICH V. G., *Phys. Lett.* **6**, 155 (1963).
13. VAN LINT V. A. J., WIKNER E. G. and MILLER P. H., Jr., Rep. No. GA-1513 (1960).
14. DANKO J. C., KILP G. R. and MITCHELL P. V., *Adv. Energy Conversion* **2**, 79 (1962).
15. FROST R. T., CORELLI J. C. and BALICKI M., *Adv. Energy Conversion* **2**, 77 (1962).

APPENDIX B

"^{125}Te Mössbauer Effect Study of Magnetic Hyperfine Structure in the Ferromagnetic Spinel $CuCr_2Te_4$"

by

J. F. Ullrich and D. H. Vincent

Physics Letters 25A, 731 (1967)

^{125}Te MÖSSBAUER EFFECT STUDY OF MAGNETIC HYPERFINE STRUCTURE IN THE FERROMAGNETIC SPINEL $CuCr_2Te_4$*

J. F. ULLRICH ** and D. H. VINCENT

Department of Nuclear Engineering, The University of Michigan, Ann Arbor, Michigan

Received 3 October 1967

The Mössbauer hyperfine spectrum of ^{125}Te has been measured in the ferromagnetic spinel $CuCr_2Te_4$. The hyperfine field was found to be 148 ± 5 kOe. The nuclear magnetic moment of the 35.6 keV excited state of ^{125}Te was determined to be + 0.74 ± 0.07 nm.

In this letter, we report on the measurement of a transferred hyperfine field at the tellurium anion site in the ferromagnetic spinel $CuCr_2Te_4$. This compound represents a unique opportunity for studying transferred hyperfine fields using Mössbauer techniques since Te is the only chalcogenide with a known Mössbauer nuclide and $CuCr_2Te_4$ is the only ferromagnetic spinel which has been successfully prepared using tellurium as an anion [1,2].

$CuCr_2Te_4$ is one of the interesting groups of chromium spinels which have shown anomalous ferromagnetic behaviour [2-4]. $CuCr_2Te_4$ has a Curie temperature T_c = 365°K [1]. The spin configuration of this particular spinel was recently investigated by neutron diffraction techniques [5]. From the results, it was concluded that $CuCr_2Te_4$ was a normal spinel with the magnetic Cr^{3+} ions occupying solely the B sites and diamagnetic Cu^+ occupying the A sites. A model proposed to describe the magnetic behaviour in the ferromagnetic spinels [2] involves a dominant exchange interaction of the 90° Cr-X-Cr superexchanges type, where X is the anion. For the $3d^3$ cations, this exchange interaction is ferromagnetic.

In this study, the magnetic hyperfine interaction at the Te anion site was investigated using the 35.6 Mössbauer gamma ray resonance in ^{125}Te. The magnetic hyperfine interaction causes the 35.6 keV $\frac{3}{2}^+$ excited state to split into four levels and causes the $\frac{1}{2}^+$ ground state to split into two levels. Since the gamma ray transition is predominantly a magnetic dipole (M1) transition, the Mössbauer pattern will consist of six lines. The relative location of the six lines in the magnetic hyperfine pattern is completely determined by $R = \mu_1/\mu_0$, the ratio of the excited state nuclear magnetic moment to the ground state nuclear magnetic moment. The ground state moment is known from nuclear magnetic resonance measurements (μ_0 = - 0.8872 nm) [6]. The excited state moment has not been determined although previous Mössbauer measurements [7,8] have definitely established the moment as positive. From theoretical considerations, the excited state moment has been estimated to be $\mu_1 \approx +$ 0.7 nm [8].

The measurements were made using a source of ^{125}Te^m (58d). The ^{125}Te^m was obtained by neutron irradiation of Te enriched to 94% in ^{124}Te. The Te was in the form of cubic PbTe which provided a single resonance line source. The $CuCr_2Te_4$ powder was embedded in acrylic plastic for use as an absorber. The powder absorber thickness was 53.5 mg/cm^2.

The 35.6 keV gamma rays were detected using a xenon-nitrogen filled proportional counter. Selection of the escape peak provided separation of the gamma ray from the intense X-ray (27.4 keV and 31.2 keV) background. The resonant absorption spectrum was obtained using a time mode Mössbauer spectrometer. Both the source and absorber were cooled to liquid nitrogen temperature for the measurements.

A typical resonant absorption spectrum is shown in fig. 1. In order to determine whether this spectrum was a partially resolved six-line spectrum due to magnetic hyperfine splitting or whether it was a two-line spectrum due to quadrupole splitting, the data were analyzed assuming the follow-

* Research supported by the National Science Foundation, Grant No. GK 871.

** Present address: Scientific Laboratory, Ford Motor Company, Dearborn, Michigan.

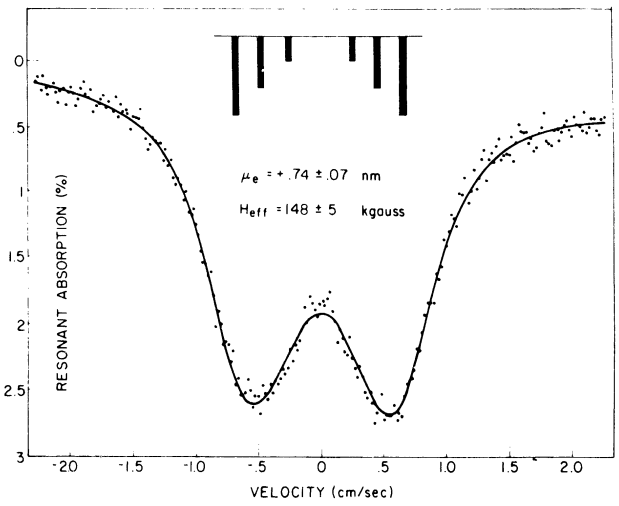

Fig. 1. Resonant absorption spectrum from a PbTe source and $CuCr_2Te_4$ obsorber (53.5 mg/cm^2) at liquid nitrogen temperature. The solid line is the "best fit" six-line spectrum. The bars denote the location and relative intensity of the six lines.

ing spectral shapes. First, it was assumed that the spectrum consisted of two Lorentzian-shaped lines with equal line widths, but different line intensities. The line locations, line intensities, and line widths were used as variables in the fitting. Second, it was assumed that the spectrum consisted of six Lorentzian-shaped lines with equal line widths. The line intensities were constrained to the ideal intensity ratio for a powder absorber (3:2:1:1:2:3 for the locations determined by $\mu_1 \approx + 0.7$ nm). The variables used in determining the line locations were R and H_{eff}, the effective hyperfine field. Other variables were the line width and a line intensity parameter. The result of the least squares computer fit with the six-line spectrum is shown as the solid line in fig. 1. The bars denote the location and relative intensity of the six lines.

On the basis of the fittings with the assumed spectra, it was concluded that the splitting was due to a magnetic hyperfine interaction. The reasons were as follows: 1) the χ^2 value for the "best fit" six-line spectrum was 25 percent smaller than the value for the two-line spectrum; 2) the line width for the two-line spectrum was 36% broader than the expected line width corrected for finite absorber thickness, whereas the line width for the six-line spectrum was in excellent agreement; and 3) the magnitude of the electric field gradient needed to produce the observed splitting ($eq = 4.3 \times 10^{16}$esu) is 10 percent greater than that due to a single 5p electron [9]. Any reasonable bonding model for Te in $CuCr_2Te_4$ would yield less than the equivalent of one unbalanced 5p electron.

In the final six-line analysis, a small quadrupole interaction was taken into account since the symmetry of the tellurium site is not cubic. The average quadrupole coupling constant obtained from the computer fit to several measurements is $\frac{1}{2}e^2qQ/ = - 0.08 \pm 0.08$ mm/sec. The average value of $R = \mu_1/\mu_0$ obtained from the data is $R = - 0.84 \pm 0.09$. Using the previously determined value of the ground state nuclear moment, we find the nuclear moment of the 35.6 keV excited state to be $\mu_1 = + 0.74 \pm 0.07$ nm, in good agreement with the estimated value. The average value of the effective hyperfine field is $H_{eff} = 148 \pm 5$kOe.

The nonmagnetic Te^{2-} ion would not normally be expected to have a hyperfine field at its nucleus. However, in a ferromagnetic compound such as $CuCr_2Te_4$, the Te 5s electrons can be spin polarized through interaction with the magnetic cations, leading to a hyperfine field at the Te nucleus through the Fermi contact interaction. The following two mechanisms are the most probable source of the polarization. First, covalent mixing of the Te 5s orbitals with the Cr 3d orbitals, and second, exchange polarization of the Te 5s electrons by the Cr 3d electrons. A 5s electron polarization of a few percent would provide a field of the right magnitude [10].

The authors express sincere thanks to C. Colominas for graciously providing the sample of $CuCr_2Te_4$.

References

1. F.K. Lotgering, in Proc. Intern. Conf. on Magnetism, Nottingham, England, 1964, 533.
2. P.K. Baltzer, P.J. Wojtowicz, M. Robbins and E. Lopatin, Phys. Rev. 151 (1966) 367.
3. P.K. Baltzer, H.W. Lehmann and M. Robbins, Phys. Rev. Letters 15 (1965) 493.
4. N. Menyuk, K. Dwight, R.J. Arnott and A. Wold, J. Appl. Phys. 37 (1966) 1387.
5. C. Colominas, Phys. Rev. 153 (1967) 558.
6. H.E. Weaver Jr., Phys. Rev. 89 (1953) 923.
7. R.B. Frankel, J. Huntzicker, E. Matthias, S.S. Rosenblum, D.A. Shirley and N.J. Stone, Phys. Letters 15 (1965) 163.
8. N. Shikazono, J. Phys. Soc. Japan 18 (1963) 925.
9. R.G. Barnes and W.V. Smith, Phys. Rev. 93 (1954) 95.
10. D.A. Shirley and G.A. Westenbarger, Phys. Rev. 138 (1965) 170.

* * * * *

APPENDIX C

"Mössbauer Measurements with K^{40}"

by

P. K. Tseng, S. L. Ruby, and D. H. Vincent

Physics Rev. 172, 249 (1968)

Reprinted from THE PHYSICAL REVIEW, Vol. 172, No. 2, 249–258, 10 August 1968
Printed in U. S. A.

Mössbauer Measurements with K^{40}†*

P. K. TSENG‡ AND S. L. RUBY
Argonne National Laboratory, Argonne, Illinois
AND
D. H. VINCENT§
University of Michigan, Ann Arbor, Michigan

(Received 1 April 1968)

This paper describes an investigation in which the 29.4-keV γ ray formed in the neutron capture reaction $K^{39}(n, \gamma)K^{40}$ was studied by use of the Mössbauer effect. Several potassium compounds were used as the neutron targets, i.e., as γ-ray sources for Mössbauer measurements. The results are: (a) All spectra show a single absorption line at $v=0$ whose width is no more than 1.3 times the minimum predicted from the lifetime; (b) the background and the recoilless fraction vary strongly from one case to another; and (c) the quadrupole splitting and isomer shifts are small if not zero. The recoilless fraction was measured as a function of temperature for a KF target. By fitting the results to curves based on a simple theory of diatomic solids, a value for the effective Debye temperature of potassium in these targets was obtained. In order to arrive at a value of $\delta\langle r^2\rangle/\langle r^2\rangle$ for the K^{40} nucleus, four careful center-shift measurements were carried out with K metal at 10°K and KF at 10, 55, and 80°K as targets, and KCl at 80°K as absorber. Comparison of these results with calculations of the thermal shifts based on our determinations of the effective Debye temperatures of the different targets shows that the measured line shifts are mainly due to thermal shifts. The accuracy of the measurements is sufficient to place an upper limit of $\delta\langle r^2\rangle/\langle r^2\rangle \leq 5\times10^{-4}$ for K^{40}.

I. INTRODUCTION

OF all nuclides with suitable properties for the Mössbauer effect, the one with lowest Z is K^{40}—but it does not have a radioactive parent. Two groups[1,2] have investigated nuclear reactions, one by (n, γ) reactions[1] and the other by (d, p),[2] as a means of forming a suitable number of excited K^{40} nuclei in an appropriate chemical or solid-state environment. The neutron-capture method proved to be the more useful one, and provided quantitative results. In particular, within the large experimental error, the result of Hafemeister and Shera,[1] using the (n, γ) reaction, showed no isomer shift between K and KF. This led to the conclusion that the fractional change of the expectation value of the squared nuclear charge radius is $\delta\langle r^2\rangle/\langle r^2\rangle < 80\times10^{-4}$.

According to Goldstein and Talmi,[3] the $f_{7/2}$ neutron

† Work performed under the auspices of the U. S. Atomic Energy Commission.

* Based on a dissertation by P. K. Tseng in partial fulfillment of the requirements for the Ph.D. degree at the University of Michigan.

‡ Permanent address: Physics Department, National Taiwan University, Taipei, Republic of China.

§ This work was partially supported by the U. S. National Science Foundation (Grant No. NSF GK 871).

[1] D. W. Hafemeister and E. B. Shera, Phys. Rev. Letters **14**, 593 (1965).

[2] S. L. Ruby and R. E. Holland, Phys. Rev. Letters **14**, 591 (1965).

[3] S. Goldstein and I. Talmi, Phys. Rev. **102**, 589 (1956).

state and the $d_{3/2}$ hole state can couple together to form four levels whose angular momenta are 4^-, 3^-, 5^-, and 2^-. This study is concerned with the first two of these. Calculations on the binding energy[4] and the magnetic moment[5] of this nucleus have been made and fit the experimental results rather accurately. Since the coupling of the states involves only the angular parts of the wave function, this model leads to the conclusion that $\delta\langle r^2\rangle/\langle r^2\rangle$ for the K^{40} nucleus will be zero—in agreement with the initial experiments.

On the other hand, a simple calculation of the electric quadrupole moment of K^{40} by coupling the Q of K^{39} with that of the extra $f_{7/2}$ neutron gives $Q_{\text{theor}}=-0.036$ b, whereas the experimental value is $Q_{\text{expt}}=-0.07$ b. Similarly, Nathan and Nilson[6] find that even in K^{39}, $Q_{\text{theor}}=+0.040$ b, while $Q_{\text{expt}}=+0.09$ b. These together suggest that the polarization of the core by the valence nucleons may be a noticeable effect, and hence that $\delta\langle r^2\rangle/\langle r^2\rangle$ in K^{40} nuclei may have a nonzero value. Moreover, nonzero values of $\delta\langle r^2\rangle/\langle r^2\rangle$ have been observed in the rotational levels of deformed nuclei[7] for which comparably rough nuclear models would also predict $\delta\langle r^2\rangle=0$.

The upper limit for $\delta\langle r^2\rangle/\langle r^2\rangle$ from the earlier experiment[1] is too large to be useful. That limit, in fact, is larger than the observed value for any known nucleus. This means that the validity of the model leading to $\delta\langle r^2\rangle/\langle r^2\rangle=0$ should be tested by more precise measurement—and this, in fact, was our major purpose.

Also it was hoped that measurements of the magnetic moment μ and the electric quadrupole moment Q for the first excited level of K^{40} would be possible by using appropriate compounds. For example, the antiferromagnetic substances $KNiF_3$ and $KCoF_3$ might have had a large transferred hyperfine magnetic field at the K nucleus and the layered structure KC_8 might have generated a measurably large electric field gradient. Finally, it was expected that measurements of the temperature dependence of the second-order Doppler shift and of the resonant fraction f would lead to information on the lattice-dynamical behavior of the potassium compounds under study.

II. TECHNIQUE

In our experiment, we chose the K^{39} (n, γ) reaction to populate the Mössbauer level in K^{40}. The reasons for choosing the (n, γ) reaction rather than the (d, p) reaction are: (1) The yield of the signal γ rays can be comparatively large for a high-intensity neutron beam (10^8 neutrons/cm^2/sec in our case); and, more important (2) since most of the neutrons (~99% in our experiment) do not interact with our necessarily thin target and most of the reaction energy escapes from the target as high-energy γ rays, the heat deposited in the target is small. Thus the target can easily be cooled. This is a big advantage over the techniques in which the Mössbauer level is populated by charged-particle reactions.

A schematic diagram of the experiment is shown in Fig. 1. A thermal-neutron beam from the reactor core emerges through collimators in the reactor shielding wall. The K^{39} target produces the signal γ ray (29.4 keV) after the neutron-capture reaction. Those γ rays are detected after passing through an absorber enriched in K^{40}. Either the target or the absorber is moved in order to perform a conventional Mössbauer transmission experiment. The first beam used was at a through hole provided with a graphite scatterer. This provided a moderate flux along with a low background. To get more time than was available at this very popular facility, we moved the experiment to a temporarily unused beam hole, which had been designed wide and thin for a neutron-mirror experiment. For this hole we built a special tapered collimator consisting of alternate layers of lead and plastic; and in its exit aperture we placed a plug of plaster containing lead and Li^6 to absorb unwanted neutrons and to minimize high-energy γ rays.

In our effort to reduce the background count of our detector in the neighborhood of the 29.4-keV line of K^{40}, we found that a considerable fraction of this background is due to scattered low-energy γ rays; these were emerging from the reactor along with the neutrons. Figure 2 shows the striking reduction of the background line when a $\frac{1}{16}$-in.-thick lead sheet was mounted before the collimator exit (as shown in Fig. 1).

A. Cryostats

Since the Debye temperature of potassium in most of its compounds is well below room temperature, it is

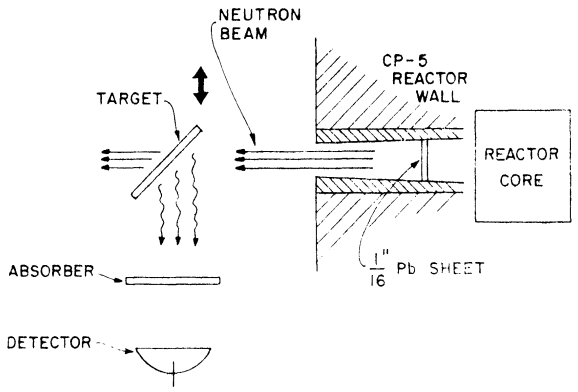

FIG. 1. Schematic diagram of the experimental setup. The double arrow shows the direction of motion of the target or absorber in the Mössbauer experiment.

[4] S. Goldstein and I. Talmi, Phys. Rev. **105**, 995 (1957).
[5] I. Talmi and S. Unna, Ann. Rev. Nucl. Sci. **10**, 353 (1960).
[6] O. Nathan and S. G. Nilson, in *α, β, and γ-Ray Spectroscopy*, edited by K. Siegbahn (North-Holland Publishing Co., Amsterdam, 1965), Chap. X, p. 618.
[7] S. Bernow, S. Devons, I. Duerdoth, D. Hutlin, J. W. Kast, E. R. Macagno, J. Rainwater, K. Runge, and C. S. Wu, Phys. Rev. Letters **18**, 787 (1967); D. Yeboah-Amankwah, L. Grodzins, and R. B. Frankel, *ibid.* **18**, 791 (1967); P. Steiner, E. Gerdau, P. Kienle, and H. T. Körner, Phys. Letters **24B**, 515 (1967).

advantageous to cool both target and absorber. (Here and in the following, "Debye temperature" is used to mean that characteristic temperature which gives the observed resonant fraction f when a monatomic Debye model is assumed for the solid.) When both target and absorber were to be kept at liquid-nitrogen temperature, the simple arrangement shown in Fig. 3 was used.

The cryostat shown here consists of a cylindrical styrofoam container E and a cover F. The space inside the container is divided into an upper and a lower part. The upper part is an aluminum can J with an annular hole; it serves as a liquid-nitrogen reservoir. The lower part, refrigerated by the cold walls of J, contains the source and the absorber.

The neutron target (source) is moved by an insulated rod C which connects through the annular hole of the can J to the moving axis of an electromechanical driver B. The thermal-neutron beam enters and leaves the cryostat directly through the styrofoam wall. The effect of the styrofoam on the neutron beam is merely to increase the background at the detector to about 10% more than that without styrofoam. This disadvantage is a small price for avoiding the difficulty of designing and handling a metal cryostat.

For some experiments the target (source) was kept at liquid-He temperature. This is necessary, especially for potassium metal, because of the very low Debye temperature of this material. For reasons of convenience, source and absorber were kept in different cryostats for these experiments, the absorber still being at liquid-nitrogen temperature. The target was mounted in the tail section of a regular liquid-helium cryostat which had been modified to allow passage of the neutron beam with minimal production of background γ radiation. The entrance and exit windows for the neutron beam had to be made fairly large and, consequently, the heat shielding of the target was not too effective. We estimate that the target temperature was $(10\pm6)°K$. Since our measurements are quite insensitive to temperature fluctuations in this range, no efforts were made to lower the temperature further or to improve the accuracy of its determination. The absorber in these experiments was kept at liquid-nitrogen temperature in a styrofoam cryostat similar to the one depicted in Fig. 3. Figure 4 shows both cryostats and the detector in their proper relative positions. Since the neutron beam is only slightly attenuated in passing through one of our cryostats, we were able to use our limited reactor time efficiently by usually running both spectrometers simultaneously, the one behind the other in the beam.

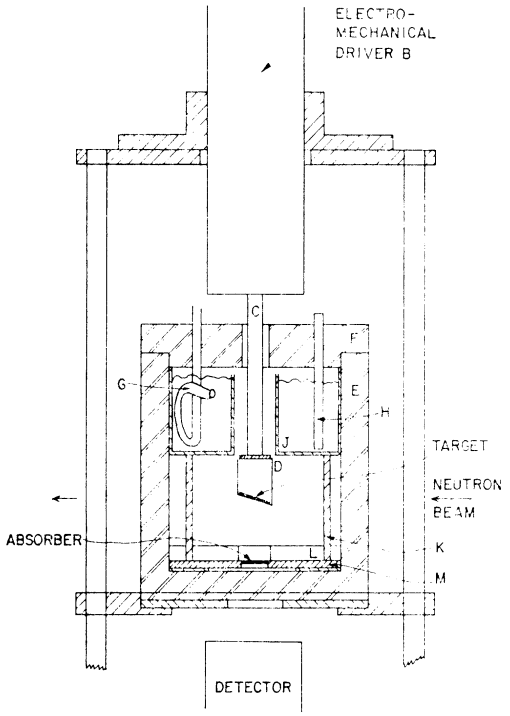

FIG. 3. Liquid-nitrogen cryostat for a Mössbauer-effect experiment with a beam of reactor neutrons. In the figure, B is the electromechanical driver, C an insulating rod connecting the driver to the target, D the target holder, G the liquid-nitrogen filling tube, H the sensing element of the automatic filling system, J the liquid-nitrogen reservoir, K the legs for J, L the neutron shielding (borated polyethylene), and M the γ shielding (lead plate).

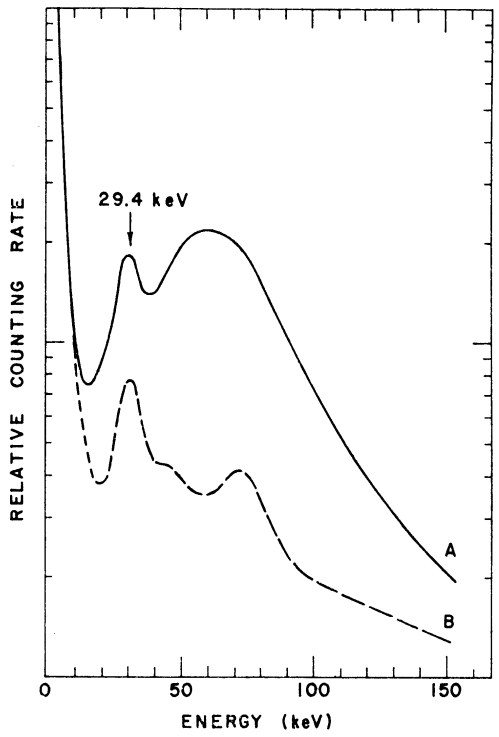

FIG. 2. γ-ray spectra detected by a 1/32-in. NaI detector. Curve A: the spectrum when the reaction is induced by an unfiltered beam of neutrons. Curve B: the spectrum when the reaction is induced by a reactor neutron beam filtered through a 1/16-in. lead sheet.

B. Mössbauer Spectrometer

When the styrofoam cryostat described in Sec. I A was used in measuring Mössbauer spectra at liquid-nitrogen temperatures, we used a standard Kankeleit-

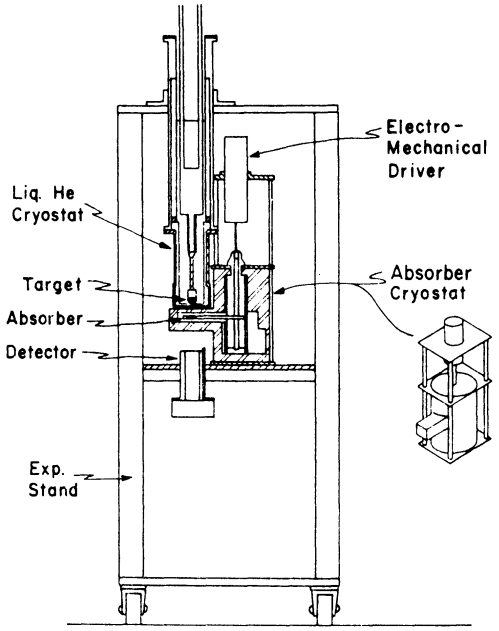

FIG. 4. Over-all experimental setup to measure the relative Mössbauer line shift between K and KF.

type[8] spectrometer (i.e., the target moved with a constant acceleration and the multichannel analyzer was in the time mode).

In measurements with the liquid-helium cryostat (Fig. 4), the moving absorber is supported by a long horizontal arm and a vertical aluminum rod. They are driven by the electromechanical driver, which is coupled to the aluminum rod by a flexible junction. Since this complexity makes the assembly somewhat flexible, it is unwise to drive this system in the constant-acceleration mode. Instead, we decided to drive the moving system sinusiodally at its resonant frequency. The reference signal for this sine wave is generated by a Hewlett-Packard model-202A function generator. In this case, the time mode of the multichannel analyzer is still used, but with a reset pulse for the address scaler derived from the function generator.

C. Targets

Since the yield of the interesting γ rays and the background are both functions of the thickness of the target, special consideration was given to the thickness of the target in order to obtain experimental results efficiently. The target thickness was usually in the range of 100–300 mg/cm^2. For some target materials, however, even optimized targets did not allow a useful experiment. For example, the compounds KI, KBr, K_2WO_3, and K_3Sb all were unusable. These difficult materials have one or more of the following properties: They contain elements with high atomic number and, consequently, have high self-absorption for the 29.4-keV γ rays from K^{40}; they contain elements which emit γ rays or characteristic x rays of energy close to 30 keV, and/or they contain nuclei with high neutron absorption cross section, in which case the K^{39} nuclei would be shielded from neutrons while at the same time a very high γ background would be produced.

After selecting a target compound and determining its optimum thickness, a disk $1\frac{1}{4}$ in. in diameter was obtained by pressing a fine powder of the compound into a mold. In some cases Lucite was used as a binder; in other cases the powder was pressed while enclosed in an aluminum foil. The latter method can give a moderately rigid disk even for noncompacting powders.

D. Absorbers

Since the natural abundance of K^{40} is only 0.0118%, it was necessary to use a sample enriched in this isotope. A KCl sample enriched to 1.9% K^{40} was obtained from Oak Ridge National Laboratory and the absorber was made by pressing the powder, with Lucite as a binder, just as in preparing the targets. The K^{40} thickness of the KCl absorber was 0.66 mg/cm^2. This gives an effective thickness $t=n\sigma f\approx 2$ at 80°K when the effective Debye temperature is taken as 180°K.

III. RESULTS AND DISCUSSIONS

A. Observations in Various Potassium Compounds

Several potassium compounds were used as targets. In particular, we selected compounds in which a magnetic field, an electric field gradient, or a variation of the s-electron density at the site of the nucleus might reasonably be expected.

All the spectra of the various potassium compounds used, either as targets or as absorbers, showed a single absorption peak whose width is no more than 1.3 times that of the one calculated from the half-life and the effective thickness. These experimental results are summarized in Table I, which lists the target material, the absorber material, the shift v_0 of the center of the Mössbauer line from $v=0$, the width β of the line, the observed amplitude α of the line, the true amplitude α_0 (corrected for background), and an effective Debye temperature Θ_D of the target material. The recoilless fraction f was calculated for these sources from the corrected dip α_0 along with the known properties of the absorber.

The fact that all the runs in Table I gave a single unshifted line indicates that (a) $\delta\langle r^2\rangle/\langle r^2\rangle$ is small and (b) the electron configuration of the potassium atom in various compounds retains its K^+ ion structure and hence does not produce large electric field gradients nor magnetic fields at the nucleus.

It should be mentioned that little, if any, evidence for radiation-damage effects is seen in these data. Since energies up to 800 eV can be given to the nucleus from

[8] E. Kankeleit, in *Mössbauer Effect Methology* (Plenum Press, Inc., New York, 1965), Vol. II, p. 47.

TABLE I. Results of experiments at liquid-nitrogen temperature. Here v_0 is the shift of the Mössbauer line from $v=0$, β is its full width at half-maximum, α is the observed amplitude of the Mössbauer line, α_0 is the true amplitude (corrected for background), and Θ_D is the Debye temperature of the target [with $\Theta_D(\mathrm{KCl})=190°$ taken as standard].

Target	Absorber	v_0 (mm/sec)	β (mm/sec)	α (%)	α_0 (%)	Θ_D (°K)
KF	KI	0.015±0.012	2.55±0.04	0.88±0.01	2.4	...
KF	KCl	−0.005±0.008	2.74±0.04	3.21±0.04	6.4	230
KCl	KCl	−0.015±0.033	3.1±0.2	0.69±0.02	2.7	190
KC_8	KCl	0.006±0.006	2.7±0.03	1.303±0.006	3.4	195
$KNiF_3$	KCl	−0.00±0.02	2.7±0.1	1.05±0.02	5.1	215
$KCoF_3$	KCl	0.01±0.03	2.9±0.1	0.60±0.01	3.9	205
KO_2	KCl	0.02±0.01	2.82±0.06	0.044±0.006	1.4	170
$KAlSi_3O_8$	KCl	−0.13±0.09	3.2±0.4	1.24±0.07	3.6	200
KN_3	KCl	0.016±0.09	2.6±0.3	0.85±0.06	2.7	190
KOH	KCl	0.01±0.04	3.0±0.2	1.88±0.05	3.0	190
KCN	KCl	−0.4±0.3	2.9±0.9	0.51±0.09	1.0	160
KH	KCl	0.05±0.04	3.2±0.3	1.42±0.05	2.7	190
KF·HF	KCl	−0.03±0.02	3.3±0.1	1.02±0.02	2.1	180

the γ-ray emission following neutron capture, it is conceivable that disruption of the lattice could affect the Mössbauer emission; a small number in the last two columns of Table I might be explained by such a mechanism. In cases in which the Debye temperatures are known approximately from other evidence (as described in Sec. III B), such radiation-damage effects are too small to be observed.

B. Measurement with a KF Target and a KCl Absorber

The target material that gives rise to the largest Mössbauer effect is potassium fluoride. With a KF target it was therefore possible to take a reasonably accurate Mössbauer spectrum in a comparatively short time (~6 h). Since the experimental equipment and techniques evolved steadily in the course of the experiment, we reran the KF-KCl measurements several times—both to take advantage of improvements and to assess their value. Thus the KF-KCl experiment became the standard test to evaluate the latest changes in the neutron collimators, shielding, detectors, etc.; the observed amplitude α of the Mössbauer line was squared and multiplied by the counting rate R to obtain the figure of merit $R\alpha^2$. Moreover, the stability of the over-all experimental system could be tested by examining the results of several runs of the same experiment. If the results fluctuate only in the anticipated statistical fashion, then the over-all experimental apparatus is functioning in a stable, reproducible manner.

In order to estimate the reproducibility of the experiment we plotted the values of v_0 for the repeated runs in chronological order, as shown in Fig. 5. Since the scatter among the several runs is not much greater than the uncertainty in each experiment, there seems to be no appreciable drift. More quantitatively, this can be shown by comparing the weighted standard deviation of the experimental points (0.007 mm/sec) with the errors of single runs (0.005–0.010 mm/sec). Comparison with similar data in the literature,[1,2] also plotted in this figure, shows the great improvements in experimental techniques that have been obtained.

C. Measurements with a KF Target and KI Absorber

According to Shirley,[9] the isomer shift can be described by the equation

$$\delta=\tfrac{2}{5}\pi Ze^2S'(Z)\langle r^2(A)\rangle[\,|\,\psi_a(0)\,|^2-|\,\psi_s(0)\,|^2]\delta\langle r^2\rangle/\langle r^2\rangle. \quad (1)$$

Here Z is the atomic number and A the atomic weight of the Mössbauer nucleus, r is its radius, $\psi_a(0)$ and $\psi_s(0)$ are the electron wave functions at the nucleus for absorber and source atom, respectively, $S'(Z)$ is a relativistic correction tabulated in Ref. 6, and the fraction $\delta\langle r^2\rangle/\langle r^2\rangle$ is the mean square fractional change in the nuclear radius as a result of the transition from the first excited state to the ground state.

The largest isomer shift δ between potassium halides would probably be that for a KF target and KI absorber, in analogy with the results of the Mössbauer experiments[10] on the Cs^{133} halides. In the latter, the isomer shift between a CsF source and a CsI absorber was found to be 0.031±0.004 mm/sec. If

$$[\,|\,\psi_a(0)\,|^2-|\,\psi_s(0)\,|^2]\delta\langle r^2\rangle/\langle r^2\rangle$$

in Eq. (1) were assumed to be the same in potassium as in cesium, the isomer shift δ between KI and KF would be expected to be 0.0025 mm/sec. The decreased shift in the potassium experiment results from the combination of several factors, including the relativistic enhancement of $|\,\psi(0)\,|^2$, the change in nuclear radius (as discussed in Ref. 9), and the atomic number. On

[9] D. A. Shirley, Rev. Mod. Phys. **36**, 339 (1964).
[10] A. J. F. Boyle and G. J. Perlow, Phys. Rev. **149**, 165 (1966).

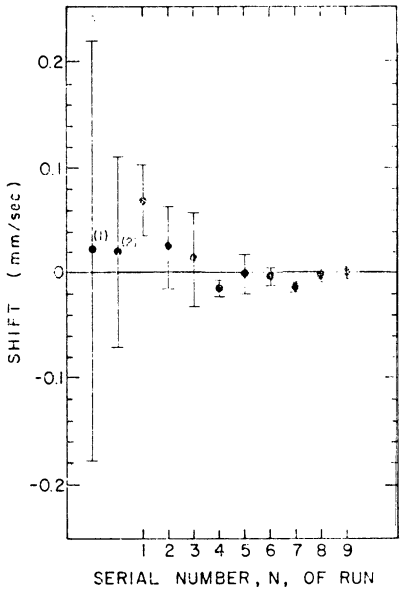

FIG. 5. Experimental values of the Mössbauer line shifts found in separate runs. The point marked (1) was taken from Ref. 1 and (2) from Ref. 2. (There is some uncertainty concerning the chemical form of the target in Ref. 2.) Other data are from the present work and are plotted in chronological order.

the other hand, the thermal shift due to the 40°K difference between the Debye temperatures of the two solids at 80°K is $v_{th}=0.01$ mm/sec. [Here we have taken $\Theta_D(\mathrm{KF})=240$°K and $\Theta_D(\mathrm{KI})=200$°K.] The experimental result for this pair of halides (Table I) is

$$v_0=0.015\pm0.012 \text{ mm/sec.} \quad (2)$$

This result indicates that the major contribution to this shift in the Mössbauer line is due to the thermal effect. Of course $\delta|\psi(0)|^2$ for these two ionic crystals is expected to be small.

D. Potassium Graphite (KC_8)

Among the various chemical compounds used as targets, potassium graphite KC_8 has the most interesting crystal structure. This is an intercalation compound[11] in which the carbon atoms form stable sheets of linked hexagons. The structure of each sheet is identical with that of graphite; but the atoms in successive carbon planes in KC_8 are in identical positions, whereas the atoms in the successive carbon planes in graphite are displaced from each other in a sequence *ABCABC* or *ABABAB*. The interplanar distance of KC_8 is 5.41 Å, whereas that of graphite is only 3.35 Å. The potassium atoms always occupy positions above or below the middle of a hexagonal ring of atoms. Each K atom gives up its outermost s electron to a conduction band. The result is that the thermal and electrical conductivity are much higher in KC_8 than in graphite.

From the point of view of the Mössbauer effect, one consequence of this is that $|\psi(0)|^2$, the electron density at the K nucleus in KC_8, may differ from that of the potassium ion. There has been a report[12] that a Knight shift has been observed in CsC_8. It is reasonable to assume that the conduction electrons in KC_8 have some s character, in agreement with the above result. A second consequence is that an electric field gradient (EFG) at the K nucleus may result from the layered structure of the graphite. This argument is supported by the observation of a splitting in the Mössbauer spectrum in cesium graphite CsC_8.[13] Unfortunately, the data on the Mössbauer effect in CsC_8 are still tentative and we are not able to make very certain judgments from these data.

Nevertheless, we made a careful Mössbauer measurement on KC_8 (as target), but the result was disappointing. The Mössbauer spectrum of KC_8 is a single line with $\beta=2.70\pm0.03$ mm/sec and $\Delta v_0=0.006\pm0.006$ mm/sec. This result shows that the quadrupole splitting is very small. The upper limit of the line broadening due to possible quadrupole splitting is less than 0.13 mm/sec. If we assume $Q_e/Q_g\approx1$, then it follows that $e^2qQ<12$ MHz.

E. Measurement of Mössbauer Line Shift between K and KF

This experiment is the main part of the work. Its purpose was to use the isomer shift of K^{40} between potassium metal and KF to evaluate the fractional difference $\delta\langle r^2\rangle/\langle r^2\rangle$ between the ground state and the first excited state.

The same KCl absorber, kept at liquid-nitrogen temperature in a separate cryostat, was used throughout these experiments. Two target materials and three temperatures were used in the four experiments. In experiment I, potassium metal was used as a target and liquid helium was used as a coolant. The same KF target was used for the other three experiments but its temperature was changed. It was maintained at 10°K by liquid helium in experiment II, at 55°K by solid nitrogen in III, and at 78°K by liquid nitrogen in IV. Experiments I and II afford a direct comparison of the line shift between K and KF.

Experiments II, III, and IV serve to check the temperature behavior of the thermal shift, from which in turn one can determine the Debye temperature for K in KF. On the other hand, we did not plan measurements on potassium metal at temperatures other than that of the liquid helium because of its extremely low Debye temperature (about 90°K). Each of the four measurements was divided into numerous equal time intervals, and the set of data obtained from each subrun

[11] W. Rüdorff, in *Advances in Inorganic Chemistry and Radiochemistry* (Academic Press Inc., New York, 1959), Vol. 1, p. 223.

[12] V. Jensen, D. E. O'Reilly, and Tung Tsang, J. Chem. Phys. (to be published).

[13] G. J. Perlow (private communication).

TABLE II. Results on the K-KF relative line-shift measurements.

Experiment No.	Target	T (°K)	α (%)	β (mm/sec)	v_0 (mm/sec)
I	K	10±6	1.26+0.05	3.32±0.13	−0.065±0.006
II	KF	10±6	7.37±0.20	3.42±0.11	−0.012±0.005
III	KF	55	4.74±0.47	3.39±0.12	0.006±0.005
IV	KF	78	4.41±0.10	3.24±0.09	0.015±0.004

was analyzed individually. The scattering of the data obtained from those subruns was no greater than the statistical error of a single subrun. These results show that the experiments were normal and reproducible.

Table II lists the results of the computer analysis of the sum of all the subruns. The values of α, β, and the relative shift v_0 to an arbitrarily selected channel are listed in the third, fourth, and fifth columns, respectively. In each case, the quoted uncertainties reflect only the statistical errors. The Mössbauer line shift between a KF source at 10°K and a K metal absorber at the same temperature is

$$v_0=0.053\pm0.008 \text{ mm/sec},$$

where a positive value of v_0 means that the source and absorber are approaching each other. This line shift corresponds to the sum of the isomer shift δ and the thermal shift v_{th}, i.e.,

$$v_0=\delta+v_{\text{th}}. \tag{3}$$

The determination of the isomer shift and, consequently, of the relative change $\delta\langle r^2\rangle/\langle r^2\rangle$ in the nuclear radius will be discussed below. Obviously, to obtain δ from our measurements of v_0, a value for the thermal shift v_{th} is needed.

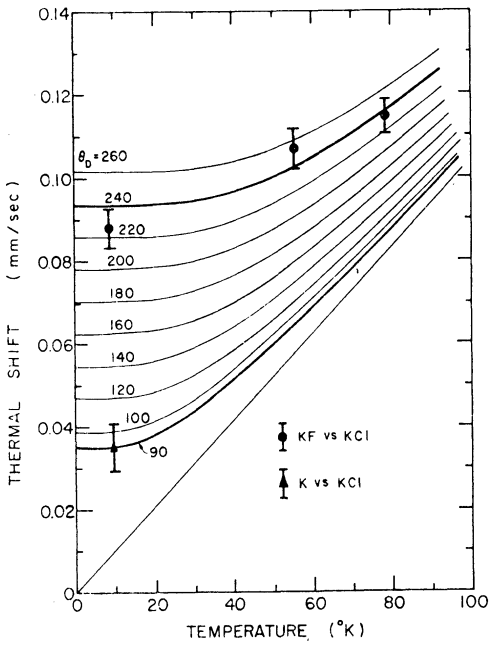

FIG. 6. Thermal shifts of KF at 10°, 55°, and 78°K and of K at 10°K. The curves were calculated relative to a fictitious absorber whose Debye temperature is 0°K and whose temperature is 0°K. Here the Debye temperature of K is assumed to be 90°K. The points for K metal and KF sources and a KCl absorber are from experiments I–IV.

The relation between the data points obtained in experiments I–IV and the Debye temperatures of K in potassium metal and in KF may be seen in Fig. 6. This figure shows how the thermal shift v_{th} in K^{40} varies with temperature for various values of the Debye temperature Θ_{Ds} of the source. The relation between the thermal shift and the temperatures of both source and absorber may be expressed[14] as

$$v_{\text{th}}=(1/2mc)[(9/8)k\Theta_{Ds}+3kT_sD(X_s) - (9/8)k\Theta_{Da}-3kT_aD(X_a)], \tag{4}$$

where

$$D(X)=\frac{3}{X^3}\int_0^X \frac{\xi^3 d\xi}{e^\xi-1},$$

and Θ_{Ds} is the Debye temperature of the source crystal, Θ_{Da} the Debye temperature of the absorber crystal, $X_s=\Theta_{Ds}/T$, and $X_a=\Theta_{Da}$.

The curves in Fig. 6 were computed from Eq. (4) by setting both Θ_{Da} and T_a equal to zero. Inspection of Eq. (4) shows that this merely suppresses an additive constant.

The data points obtained from experiments I–IV were superimposed on this graph by choosing $\Theta_{Ds}=90$°K for potassium metal on the basis of the specific-heat measurement.[15] After this choice, the position of the KF data points are automatically determined. They seem to group very nicely around the curve with the parameter $\Theta_{Ds}=240$°K. The mean deviation of these points is less than the experimental error.

F. Measurement of the Recoilless Fraction as a Function of the Source Temperature

It is impossible to determine the isomer shift between K and KF unless the thermal shift between K and KF is known. Therefore an experiment was planned to confirm our earlier measurements of the Debye temperature of KF.

[14] R. V. Pound, in *Proceedings of the International Conference on the Mössbauer Effect, Saclay, France, 1961*, edited by D. M. J. Compton and A. H. Schoen (John Wiley & Sons, Inc., New York, 1962), p. 222.

[15] L. M. Roberts, Proc. Phys. Soc. (London) **B70**, 744 (1957).

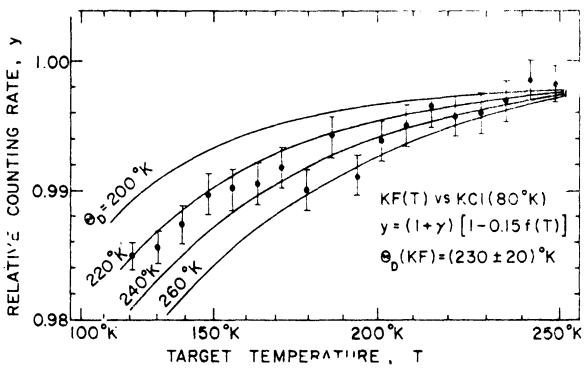

FIG. 7. The experimental results (points) on the recoilless fraction $f(T)$ as a function of the target temperature. The target is KF. The curves give the calculated relative transmission $y(T)$, through the Mössbauer absorber with known effective thickness. In addition, the background ratio is given by a separate measurement. These calculated curves have then been shifted along the y axis a small amount γ to fit the experimental data.

The experiment is the measurement of the counting rate $R_{v=0}$ of the transmitted γ ray as a function of the temperature of the target. The rate $R_{v=0}$ depends on the temperature in accordance with the relation[5]

$$R_{v=0}(T)=R_{\mathrm{BG}}+R_s e^{-\mu t}\{1-f_\Theta(T)[1-e^{-\frac{1}{2}t_e}J_0(\tfrac{1}{2}it_e)]\}, \tag{5}$$

where R_{BG} is the counting due to the background and does not depend on the presence of the absorber, R_s is the counting rate of the resonant γ ray when the absorber is not present, t is the thickness of the absorber, μ is the γ-ray attenuation coefficient of the absorber material at 29.4 keV, $f_\Theta(T)$ is the recoilless fraction of the emitted 29.4-keV γ ray from the target at temperature T and Debye temperature Θ_D, and t_e is the effective thickness of the absorber for the Mössbauer γ ray. After dividing $R_{v=0}$ by its temperature-independent part, we find that the reduced function $y(T)$ is

$$y(T)=R_{v=0}(T)/(R_{\mathrm{BG}}+R_s e^{-\mu t})=1-c_0 f_\Theta(T), \tag{6}$$

where

$$c_0=n_s e^{-\mu t}/(R_{\mathrm{BG}}+R_s e^{-\mu t})[1-e^{-\frac{1}{2}t_e}J_0(\tfrac{1}{2}it_e)]. \tag{7}$$

In Eq. (6), c_0 can be calculated from the information on the signal-to-background ratio and on the equivalent resonant thickness t_e of the absorber. Then $y(T)$ can be calculated numerically for a particular Debye temperature. To measure $y(T)$ experimentally, the source and absorber were kept at rest with respect to each other and each temperature interval (from T to $T+\Delta T$) was associated with a particular channel I of the multichannel analyzer. Counts were simultaneously accumulated in two halves of the analyzer—one half accumulating the count $n_r(I)$ from the resonant γ ray, the other accumulating the count $n_0(I)$ from a nonresonant part of the γ-ray spectrum. Then $y_{\mathrm{expt}}(T)$ is obtained from

$$y_{\mathrm{expt}}(T)=C[n_r(I)/n_0(I)],$$

where C is a parameter to be adjusted to fit the properties of Eq. (6), i.e.,

$$\lim_{T\to\infty} y_{\mathrm{expt}}(T)=1, \tag{8}$$

$$y(T_0)=y_{\mathrm{expt}}(T_0)=1-c_0 f(T_0)=1-\alpha. \tag{9}$$

Equation (8) means that the resonant absorption will vanish when the temperature of the source is considerably higher than the Debye temperature; and Eq. (9) means that y is equal to one minus the amplitude α of the resonance peak when a Mössbauer spectrum is taken at temperature T_0.

In practice, C is replaced by $C'/(1+\gamma)$, where C' is a constant obtained by a rough estimate from the relations (8) and (9), and γ is a parameter to be adjusted when the y_{expt} points are fitted to the value of $y(T)$ calculated for each Debye temperature by use of Eq. (6).

The fitting was done graphically, by making use of the strong variation of the curvature of $y(T)$ with Θ_D. The resultant best fit for the KF target is

$$\Theta_D=(230\pm 20)^\circ\mathrm{K}.$$

Figure 7 shows the experimental points and the fitting curves for the case of KF versus KCl. Each experimental point is the average of ten analyzer channels.

The importance of this result to the final accuracy of the $\delta\langle r^2\rangle/\langle r^2\rangle$ measurement was not reflected in the duration of this experimental run. The quoted uncertainty of $\pm 20^\circ$K could have been reduced by a factor of four by running for several days instead of several hours. At the time these data were taken, it was assumed that an accurate value of Θ_D could be obtained from specific-heat data on KF.

G. Estimation of the Debye Temperatures of K and KF

As was mentioned in the discussion of Eq. (3), a value for the thermal shifts of both K and KF would permit us to obtain the isomer shift between these two materials from our measured value of the relative Mössbauer line shift between K and KF.

Equation (4) gives the relation between the thermal shift and the Debye temperatures of both the source and the absorber. In the following we discuss our choices for Θ_D for potassium metal and KF, which we used for the determination of the thermal shifts between these two substances. All relevant data are assembled in Table III.

Our single determination of the Debye temperature

of potassium metal was made by computing it from the single observed amplitude of the Mössbauer resonance line. This value is

$$\Theta_D(K) = (90\pm8)°\text{K}.$$

For confirmation of this value we may look to Θ_D values extracted from specific-heat measurements.[15] In the range from $0<T<20°$K, these values drop from 90° down to 83° and return to 95°. We feel that our experimental value for the Debye temperature should be compared with the specific-heat result[15] at 0°K, namely (89.1±5)°K.

As seen in Table III, four different values for the Debye temperature of KF were obtained by different methods in the present work. The weighted mean of these four Debye temperatures is

$$\Theta_D(\text{KF}) = (236\pm20)°\text{K}.$$

The Debye temperatures obtained from the previous Mössbauer experiment[1] differ moderately from our result. It seems that their results are strongly dependent on the precise determination of the background in the pulses from the single-channel analyzer. In their experiment, this background was not measured, but only estimated from the shape of the γ-ray pulse-height spectra. In our case, the γ-ray spectra were studied as a function of attenuation in lead absorbers with thicknesses ranging from zero to 120 mg/cm². This provided a better criterion by which 29.4-keV pulses due to γ rays emitted by the target could be distinguished from those created in the detector itself. In our further analysis, the effective Debye temperatures from Ref. 1 will not be used. In addition, we were surprised to find no precise specific-heat data for KF. Therefore the above-mentioned weighted mean of the four effective Debye temperatures from the present work is used.

TABLE III. Estimate of the Debye temperatures of K and KF from various methods.

Target material	Method of measurement	T (°K)	Θ_D (°K)	Ref.
K	α (amplitude of the Mössbauer line)	10±6	90±8	a
K	α	4	60±(?)	b
K	Specific heat	0	89.1±0.5	c
KF	α	78	235±20	d
KF	$\alpha(10)/\alpha(78)$	10, 78	247±25	e
KF	$f(T)$ (recoilless fraction)	100–200	230±20	a
KF	v_{th} (thermal shift)	10, 55, 78	205±55	a
KF	α	4	145±(?)	b
KF	α	78	190±(?)	b

[a] Present work.
[b] D. W. Hafemeister and E. B. Shera, Phys. Rev. Letters **14**, 593 (1965).
[c] L. M. Roberts, Proc. Phys. Soc. (London) **B70**, 744 (1957).
[d] Present work. See Table I.
[e] Present work. The data used for the calculation of the Debye temperature were taken from Table II.

H. Estimate of the Isomer Shift between K and KF and of $\delta\langle r^2\rangle/\langle r^2\rangle$ for K^{40}

For the reasons explained in Sec. III G, the Debye temperatures have been taken to be

$$\Theta(\text{K}) = (90\pm8)°\text{K} \quad \text{for} \quad \text{K},$$

$$\Theta(\text{KF}) = (236\pm20)°\text{K} \quad \text{for} \quad \text{KF}.$$

When these data are substituted in Eq. (4), the thermal shift v_{th} between KF and K is found to be

$$V_{\text{th}} = 0.055\pm0.009 \text{ mm/sec}.$$

Then by Eq. (3), the isomer shift δ is

$$\delta = v_0 - v_{\text{th}} = -0.002\pm0.012 \text{ mm/sec}. \qquad (10)$$

Equation (1) is a relation between δ and $\delta\langle r^2\rangle/\langle r^2\rangle$. This relation becomes simple after substituting the numerical data. Then according to Shirley,[9] the shift in mm/sec is

$$\delta = (1/0.0214)\Delta\,|\psi(0)|^2\delta\langle r^2\rangle/\langle r^2\rangle, \qquad (11)$$

where $\Delta\,|\psi(0)|^2$ is the difference between the s-electron density in K and that in KF in atomic units (i.e., in units of a_0^{-3}, where $a_0 = 0.52918\times10^{-8}$ cm). Since our upper limit on the shift is $\delta \leq 1.2\times10^{-2}$ mm/sec, it follows that

$$\delta\langle r^2\rangle/\langle r^2\rangle \leq (2.66\times10^{-4})/\Delta\,|\psi(0)|^2, \qquad (12)$$

where $\Delta\,|\psi(0)|^2$ can be calculated theoretically. As a first approximation to the charge-density difference between the potassium ion and the metal, the charge density due to a $4s$ electron in a free potassium atom will be used. This neglects the (probably small) effect of the rearrangement of the inner electrons in the K^+ ion. Shirley[9] gives $|\psi_{4s}(0)|^2 = 1.11$ per atomic volume for $4s$ electrons. This value agrees with the value [($|\psi_{4s}(0)|^2 = 1.06$ per atomic volume] calculated on the basis of the results of Skillman and Herman.[16]

By using Hartree-Fock calculations with an improved method for electron correlations, Wilson[17] obtained the difference between the value of $|\psi(0)|^2$ for a free potassium atom and a free K^+ ion. This result is 0.76 per atomic volume. Since Wilson's method seems to be a better approximation to physical reality, his value will be used for further calculation.

[16] S. Skillman and F. Herman, *Atomic Structure Calculation* (Prentice-Hall, Inc., Englewood Cliffs, N. J., 1963).
[17] M. Wilson (private communication).

For a second approximation, the difference between the free atom and the metal must be considered. The density $|\psi(0)|^2$ of $4s$ electrons in pure K metal is complicated to calculate. Most of the band-theory calculations are done with no particular interest in the behavior near the nucleus, and the pseudopotential calculations are completely useless for the present purpose. Shirley[9] has presented reasons for believing that a better approximation might be obtained by taking $|\psi(0)|^2=0.7|\psi_a(0)|^2$, the electron densities at the nucleus being $|\psi(0)|^2$ for the s electrons of the conduction band and $|\psi_a(0)|^2$ for the $4s$ electrons in a free atom.

In the light of this discussion, the most reliable value for $\Delta|\psi(0)|^2$ would be 0.7 times the value calculated by Wilson.[18] Then the upper limit of $\delta\langle r^2\rangle/\langle r^2\rangle$ is

$$\delta\langle r^2\rangle/\langle r^2\rangle<5.0\times10^{-4}.$$

IV. CONCLUSION

The conclusion at the end of Sec. III H was that $\delta\langle r^2\rangle/\langle r^2\rangle$ for the K^{40} nucleus must be quite small and that, with some confidence, its upper limit can be given as

$$\delta\langle r^2\rangle/\langle r^2\rangle<5.0\times10^{-4}.$$

This result indicates that the simple vector-coupling calculation of $\delta\langle r^2\rangle/\langle r^2\rangle$ for the K^{40} nucleus, which gives exactly zero, is still true within the uncertainty 5×10^{-4}.

In using this result, one should keep in mind the various measurements, parameters, and assumptions on which we have based our estimate of $\delta\langle r^2\rangle/\langle r^2\rangle$. These are: (a) The over-all Mössbauer line shift between K and KF at liquid-helium temperature was measured to be 0.053 ± 0.008 mm/sec. (b) Potassium metal is assumed to be a Debye solid with an effective Debye temperature equal to 90 ± 8°K at liquid-helium temperature. (c) Similarly, KF has an effective Debye temperature equal to 236 ± 20°K at liquid-helium temperature. (d) The value for the difference $\Delta|\psi(0)|^2$ between the electron densities at the nuclei of K and KF was based on (1) Wilson's calculation[18] of the difference $\Delta|\psi(0)|^2$ between a free potassium atom and a free K^+ ion and (2) a correction factor defined as the ratio ξ' of the wave function for the $4s$ electrons in the conduction band of potassium metal to the wave function for the $4s$ electrons in a free potassium atom, both wave functions being evaluated at the nucleus. (We used $\xi'=0.7$ as suggested by Shirley.[9])

[18] Y. Nisatnik, D. Fainstein, and H. J. Lipkin, Phys. Rev. **139**, A292 (1965).

Note especially that the usefulness of increasing the accuracy of measurement a is severely limited by the present uncertainty in assumptions b and c. No precise Debye temperature of KF is available. In any case, a Debye solid is only a first-order approximation to a real crystal. Moreover, even if one could get precise data on the internal energy of K and KF, the lack of a precise and practical theory to deduce useful values from these data would still render the Debye temperature uncertain. (For example, the Debye temperature computed from the specific-heat data on KF needs to be modified[18] before it can be used as the Θ_D in the Mössbauer effect.) In addition, the induced radiation damage due to the preceding high-energy γ-ray emissions of the target nuclei may limit the direct application of the reduced internal energy to the target crystal. For these reasons, we conclude that our measurement is the best that can be justified so far, and that more accurate measurements on δ will have no physical significance unless the uncertainty in the thermal shift can be overcome by both theoretical and experimental efforts.

It should be pointed out that the measurements reported here for $f(T)$ are by no means at their limits of accuracy. Therefore, although it does seem clear that little useful chemical or magnetic information can be found by use of the Mössbauer effect in K^{40}, lattice dynamical measurements utilizing potassium do seem to be practical. For example, it may be profitable to study the ferroelectrics KH_2PO_4 or $K_2Fe(CN)_6\cdot3H_2O$ with this technique.

ACKNOWLEDGMENTS

We would like to thank G. J. Perlow, R. S. Preston, and G. M. Kalvius for their constant advice and encouragement. We also wish to thank the neutron measurements group for use of the H-1 beam hole and G. R. Ringo and V. Krohn for use of the H-13 hole.

Special thanks go to B. J. Zabransky for his clever help in the construction and maintenance of some of the apparatus and for his diligent help with the computer program. We also appreciate the kind help of the operating staff of the CP-5 reactor at Argonne and of the Ford Nuclear Reactor at the University of Michigan during the neutron-beam experiments.

For their help in the special arrangements to make possible their research at Argonne National Laboratory, one of the authors (P. K. T) is grateful to L. M. Bollinger of Argonne and to W. Kerr of the University of Michigan. In addition, he wishes to thank K. H. Sun for suggesting this combined program of study at Michigan and research at Argonne.

APPENDIX D

"A New Method for the Analysis of Temperature Dependent Quadrupole Splitting in Mössbauer Spectra"

by

P. B. Merrithew, P. G. Rasmussen, and D. H. Vincent

Submitted for publication

A New Method for the Analysis of Temperature Dependent Quadrupole Splitting in Mossbauer Spectra*

P. B. Merrithew, P. G. Rasmussen
Chemistry Department, The University of Michigan
and D. H. Vincent
Nuclear Engineering Department, The University of Michigan

Abstract

A new method for the analysis of temperature dependent quadrupole splitting in Mossbauer spectra has been developed. Accurate quadrupole splitting data has been obtained for the compounds $Fe(py)_4Cl_2$ (py = pyridine), $Fe(py)_4I_2$, $Fe(py)_4I_2 \cdot 2py$ $Fe(py)_4(SCN)_2$, $Fe(NH_4SO_4)_2 \cdot 6H_2O$, $Fe(phen)_3(ClO_4)_3$ (phen = 1,10 phenanthroline), and $K_3Fe(CN)_6$ in the region 100° to 300°K. A plot of $\ln(|Q.S.^\circ - Q.S.|)$ vs $1/T$ (Q. S. = quadrupole splitting, Q.S.° = low temperature maximum quadrupole splitting) is found to be linear in most of the cases studied. This implies that these compounds can be well described as a two state system over this temperature range. The high temperature intercept ($|Q.S._e|$) is the quadrupole splitting expected from the totally populated excited state and is independent of the so called lattice contribution to the quadrupole splitting. It is concluded from the results that spin orbit coupling effects have previously been overestimated and covalency effects underestimated.

I. Introduction

In Mossbauer spectroscopy experiments high spin Fe^{2+} and low spin Fe^{3+} compounds normally show relatively large, temperature dependent, electric quadrupole splittings. These large splittings and their temperature dependence are due to the presence of an uncompensated 3d electron.

For Fe^{57m} the quadrupole splitting is given by

$$Q.S. = 1/2\ e^2\ qQ[1 + 1/3\ \eta^2]^{1/2}$$

where Q is the quadrupole moment of Fe^{57m} and q and η are expressed in terms of the components of the electric field gradient tensor (e.f.g.) at the nucleus. When the principal axes have been chosen so that $|V_{zz}| \geq |V_{yy}| \geq |V_{xx}|$, $q = V_{zz}/e$ and $\eta q = (V_{xx}-V_{yy})/e$. Assuming an ionic model these quantities can be written

$$q = (1-R)\ q_{val} + (1-\gamma_\infty)\ q_{lat}$$

$$\eta q = (1-R)\ \eta_{val}\ q_{val} + (1-\gamma_\infty)\ \eta_{lat}\ q_{lat}$$

where the subscript val refers to the charge distribution of the uncompensated 3d electrons of the metal ion and the subscript lat refers to the charge distribution of the neighboring ions. The Sternheimer factors,[1,2] (1-R) and $(1-\gamma_\infty)$ are included to account for the polarization of the electron core.

In octahedral symmetry the appropriate metal ion eigenfunctions are[3]

$$t_{2g}^{\circ} = 1/2\ (d_2-d_{-2})$$

$$t_{2g}^{-} = d_{-1}$$

$$t_{2g}^{+} = d_1.$$

The contribution to the e.f.g. from a single electron occupying these orbitals can be obtained by calculating the appropriate expectation values[4]:

$$\text{for } t_{2g}^{\circ},\ V_{zz}/e = 4/7\langle r^{-3}\rangle$$
$$\text{for } t_{2g}^{-},\ V_{zz}/e = -2/7\langle r^{-3}\rangle$$
$$\text{and for } t_{2g}^{+},\ V_{zz}/e = -2/7\langle r^{-3}\rangle.$$

η_{val} is zero for these wave functions. If the lattice contributions to the e.f.g. can be considered not to effect the orientation of the major axes of the e.f.g. tensor then, because all of these wave functions have the same major axis, the quadrupole splitting may be treated as a scalar. For example, the temperature dependence of the quadrupole splitting for a Fe^{2+} high spin, purely ionic, compound with a small axial distortion can be approximated by:

$$(t_{2g}^{\circ} \text{ ground orbital})$$
$$Q.S. = Q.S._{lat} + K4/7\langle r^{-3}\rangle + 2K(-2/7)\langle r^{-3}\rangle \exp -\Delta E/kT$$

and

$$\ln(Q.S.^{\circ} - Q.S.) = \ln(K4/7\langle r^{-3}\rangle) - \Delta E/kT$$

where

$$Q.S.^{\circ} = Q.S._{lat} + K4/7\langle r^{-3}\rangle \quad \text{and } K = 1/2\ e^2Q$$

A plot of $\ln(Q.S.^{\circ} - Q.S.)$ vs $1/T$ will be linear with intercept of $K4/7\langle r^{-3}\rangle$.

In a real case covalency effects must be considered. These effects can be thought to produce an expansion in the radial part of the wave function and hence will reduce the Q.S. contribution from each state. Since in general this effect will

not be the same for each state we will designate the Q.S. produced by the totally populated ground and excited state as $Q.S._g$ and $Q.S._e$ respectively. In addition to $Q.S._{lat}$ another temperature independent contribution must be included due to anisotropy in bonding to the orbitals occupied by the compensated 3d electrons. We will call the sum of these effects $Q.S._{lig}$. With the additional assumption that the covalency effects do not alter the major axes of the e.f.g., then, we can write for the above case:

$$\ln(Q.S.^\circ - Q.S.) = \ln(-Q.S._e) - \Delta E/kT$$

where

$$Q.S.^\circ = Q.S._{lig} + Q.S._g.$$

For the experimental case when only the magnitude of the Q.S. is known we write

$$\ln(|Q.S.^\circ - Q.S.|) = \ln(|Q.S._e|) - \Delta E/kT.$$

This expression is a phenomenological description of the parameters, whose validity will be demonstrated empirically by the data below. A good straight line fit to a plot of $\ln(|Q.S.^\circ - Q.S.|)$ vs $1/T$ will also imply a two state system.

II. Experimental Details

The compounds $Fe(py)_4Cl_2$, $Fe(py)_4I_2$, $Fe(py)_4I_2 \cdot 2py$ and $Fe(py)_4(SCN)_2$ (py = pyridine) were prepared according to the methods of Golding, Mok and Duncan.[5] The room temperature Q.S.

results for $Fe(py)_4Cl_2$ and $Fe(py)_4(SCN)_2$ agreed with those of the above authors. The room temperature Q.S. values for $Fe(py)_4I_2$ and $Fe(py)_4I_2 \cdot 2py$ were about 0.3 mm/sec smaller. The absence of third peaks confirm the purity.

The compound $Fe(phen)_3(ClO_4)_3$ (phen = 1,10 phenanthroline) was prepared by the slow addition of nitric acid to a $Fe(phen)_3^{2+}$ solution until the solution turned blue. Excess $NaClO_4$ was added and the solution allowed to stand for twelve hours. The crystals which formed were filtered and dried. The room temperature Q.S. obtained agrees with that of Erickson.[6]

The $Fe(NH_4SO_4)_2 \cdot 6H_2O$ was Merck reagent. The $K_3Fe(CN)_6$ was Mallinckrodt reagent.

The Mossbauer drive is described elsewhere.[7] The spectra were analyzed with a Fortran IV translation of a Michigan Algorithm Decoder (MAD) program described elsewhere.[7] The errors are determined statistically by the computer program. The results are found to be normally reproducible within the stated error. The accuracy is 1%.

The dewar consisted of an aluminum sample holder fastened beneath a liquid nitrogen reservoir with a thermal resistor. Heating wire was wound above the sample holder. The whole apparatus was insulated with styrofoam. Variation of the thermal resistors and the heating current allowed temperature control in the range of 100° - 300° K. The temperature was measured with a Cu - Constantan thermocouple. The temperatures are accurate to $\pm$ 0.5°.

III. Results and Discussion

The data is shown in Table I. A typical spectrum is shown in Figure 1. Since our data was confined to the region above 100°K, Q.S.° could not be directly determined. Estimation of Q.S.° was simple for the compounds $Fe(py)_4(SCN)_2$, $Fe(py)_4I_2$, $Fe(py)_4I_2 \cdot 2py$, $Fe(py)_4Cl_2$ and $Fe(phen)_3(ClO_4)_2$ since by 100°K the Q.S. has become nearly independent of temperature. Choice of Q.S.° for $K_3Fe(CN)_6$ and $Fe(NH_4SO_4)_2 \cdot 6H_2O$ is more difficult. These values were chosen to give a linear plot. Our predicted value for $|Q.S.°|$ for $K_3Fe(CN)_6$ of 0.535 mm/sec agrees quite well with the value of 0.524 mm/sec obtained by Oosterhuis, Lang and de Bendetti.[8] Their Q.S. value at 77°K fits on the linear plot.

The plots are shown in Figures 2 to 8. The data on all these compounds, except $Fe(py)_4I_2$ and $Fe(NH_4SO_4)_2 \cdot 6H_2O$, is described by equation 2. The plot for $Fe(py)_4I_2$ definitely is not linear. Because of the uncertainty in Q.S.° for $Fe(NH_4SO_4)_2 \cdot 6H_2O$ it is possible that this compound exhibits non-linear behavior at low temperatures. From the rate of change of the Q.S. at 100°K we estimate that $|Q.S.°| = 2.76$ to 2.96 mm/sec and $|Q.S._e| = 3.40$ to 3.64 mm/sec. The ΔE value obtained from the slope of the linear plot for this compound thus represents an upper limit.

A. Spin Orbit Coupling

An axial field splits the $^5T_2$ ground term of high spin Fe^{2+} into a $^5B_2$ and a degenerate ^5E state. The combined effect of an

axial field and of spin orbit interaction on a cubic $^5T_2$ term produces nine levels.[9] The free ion value of the spin orbit coupling constant λ is 148°.[10] Because three of the five high spin Fe^{2+} compounds considered here can be described well as two state systems in the region below room temperature, it appears that the effects of spin orbit coupling are relatively minor. Eibschutz, Ganiel and Shtrikman[11] fit their data obtained for the compound, $FeNb_2O_6$, and conclude that $\lambda = 90°$. This value of λ results in a splitting of the excited level of about 300°. Since our compounds show crystal field splittings of 500° to 600°, a value of λ as large as 90° is inconsistent with the simple two state analysis of these systems. Their conclusion of a large spin orbit coupling constant probably results from their assumptions of axial symmetry and zero $Q.S._{lig}$.

Spin orbit coupling mixes the t_{2g} wave functions and therefore should reduce the values of $|Q.S._e|$ and $|Q.S._\eta|$. Consider the results obtained for the compound $Fe(NH_4SO_4)_2 \cdot 6H_2O$. On the basis of Ingalls' treatment of spin orbit mixing,[12] a compound with free ion spin orbit coupling and an axial splitting of 380°, should have $|Q.S._e|$ and $|Q.S._\eta|$ values at least 50% reduced from those values observed in a compound with very large ΔE. $Fe(NH_4SO_4)_2 \cdot 6H_2O$, however, has the largest value for $|Q.S._e|$ of the compounds studied but has the smallest axial splitting. $|Q.S._e|$ for this compound (3.44 - 3.64 mm/sec) is nearly as large as the Q.S. observed for the compound $FeSiF_6 \cdot 6H_2O$ (3.67 mm/sec)[13,14] which has a ΔE of about 1200 cm^{-1}.[15,16] This compound has the largest Q.S. known. It is likely that the large Q.S., compared

to other $Fe(H_2O)_6^{2+}$ salts, arises because the $Q.S._{lig}$ contribution happens to augment the $Q.S._g$. Spin orbit mixing in the compound $Fe(NH_4SO_4)_2 \cdot 6H_2O$ must then be considered negligible. For spin orbit coupling effects to be negligible, (reduction in Q.S. less than about 10%) the effective spin orbit coupling constant must be less than 40°.

The combination of an axial field and spin orbit coupling removes the degeneracy of the ground cubic $^2T_2$ state of low spin Fe^{3+}.[17] Since the data on $K_3Fe(CN)_6$ indicates that to a good approximation the cubic $^2T_2$ state has been split into only two states, it must be concluded that either the axial field or spin orbit effects are minor. The values of $|Q.S._\circ|$ and $|Q.S._e|$ are not equal indicating that the CN^- bonding is not isotropic. The splitting ΔE observed here is therefore due to ligand asymmetry. An exact value for the spin orbit coupling constant in this compound cannot be obtained without accurate low temperature data. The spin orbit coupling constant is related to the splitting of the ^2E state and is therefore related to the deviation from linear behavior at low temperatures. We estimate that the spin orbit coupling constant must be less than 60° since a splitting of this magnitude would be easily detected in the temperature range we have studied. This value is at considerable variance with the value of 575° derived from susceptibility data.[17]

B. Discussion of the Results for Individual Compounds

Table II shows the expected values for Q.S.° and $Q.S._e$ in the absence of covalency factors and lattice contributions for Fe^{2+} high spin and Fe^{3+} low spin compounds. In the absence of anisotropic covalency factors the ground and excited levels can be easily identified. Consider a Fe^{2+} high spin compound with axial symmetry and a ground t_{2g}° orbital (case 1, Table II). In the approximation that $|Q.S._g| = |Q.S._e|$ then Q.S.° + $Q.S._e$ = $Q.S._{lig}$ and $Q.S._{lig}$ is of the same order of magnitude as (or smaller than) the splittings observed for Fe^{3+} high spin compounds. Consider a Fe^{3+} low spin compound with t_{2g}- ground orbital t_{2g}° excited and t_{2g}^{+} much higher in energy (case 7). Here Q.S.° + 1/2 $Q.S._e$ = $Q.S._{lig}$ and $Q.S._{lig}$ should be the same order of magnitude as the Q.S. observed for similar Fe^{2+} low spin compounds. The quadrupole splittings for high spin Fe^{3+} and low spin Fe^{2+} seldom exceed 0.6 mm/sec.

Consider the compound $Fe(NH_4SO_4)_2 \cdot 6H_2O$. The ground orbital is t_{2g}° and the first excited level a (to the first approximation) degenerate (t_{2g}^{+}, t_{2g}^{-}) pair. The predicted positive sign for V_{zz} of the ground state agrees with that which has been previously determined.[18] $Q.S._{lig}$ is negative and its magnitude is between 0.6 and 0.9 mm/sec. A $Q.S._{lig}$ as large as 0.9 mm/sec is unlikely. Thus the symmetry for this compound is not precisely axial and the Q.S.° assumed to give the plot shown is somewhat small.

The compound $Fe(phen)_3(ClO_4)_3$ is described by case 7. $Q.S._{lig}$ for this compound is $\sim$2 mm/sec, of the same magnitude as the Q.S.'s

observed for Fe^{2+} low spin compounds with similar ligands.[6,19] The sign of V_{zz} for the ground state of this compound is predicted to be positive. The relatively small Q.S.° here is seen to be primarily due to the nature of the electronic structure and not due to covalency effects as has been previously suggested.[20] $Fe(py)_4(Cl)_2$ is described by case 1. $Q.S._{lig}$ here is + 0.5 mm/sec. The positive sign indicates that the compound is probably cis. The reduction in the $|Q.S._e|$ value for this compound is expected since pyridine and chloride ion are stronger π bonding ligands than H_2O.

Assignment of the energy levels in $K_3Fe(CN)_6$ is clouded by uncertainty in the strength of the strong π bonding ligand CN^- Comparison of the results for this compound with the results obtained for similarly coordinated iron in other compounds[21] indicates that this compound has a ^2E ground state. Q.S.° and $|Q.S._e|$ have been reduced by at least 70% by π bonding. This reduction is substantially greater than that estimated by Golding.[20]

The orbital level system cannot be unambiguously defined for the compounds $Fe(py)_4I_2 \cdot 2py$, $Fe(py)_4I_2$ and $Fe(py)_4(SCN)_2$ because the possibility exists for substantial anisotropic π bonding. For example, for case 1 the difference Q.S.° + $Q.S._e$ may be larger than in previous cases because $Q.S._g$ is reduced by π bonding more than $|Q.S._e|$. The compound $Fe(py)_4(SCN)_2$ is known to be trans.[22] Because the molecular and orbital major axes would be expected to be colinear in such a case, $Q.S._{lig}$ is negative. A likely level arrangement is as case 4 and a negative $Q.S._{lig}$ of 0.5 mm/sec augments the $Q.S._g$ contribution to give the larger $|Q.S.°|$. It is

possible, however, that the level system is described by case 1 and that the combination of a negative $Q.S._{lat}$ and relatively delocalized ground state produce the reduced Q.S.°.

The temperature dependence for the compound $Fe(py)_4I_2$ is particularly interesting. The small room temperature quadrupole splitting observed for this compound is not due to a small ΔE as concluded by other authors[5] but must be due to a large π interaction with I^-. The non-linearity of the plot for this compound prevents explicit determination of $|Q.S._e|$. $Q.S._e$, however, has about the same absolute magnitude as Q.S.°, indicating that the three t_{2g} orbitals show approximately equal ligand interactions. Evidently the strong π donating interaction of the I^- ions promotes stronger π acception by the pyridine. This indicates that the various bonding properties of a ligand cannot be considered independent of the compound.

The compound $Fe(py)_4I_2 \cdot 2py$ might be described by case 4 and a positive $Q.S._{lig}$ or case 1 with the small Q.S.° being due to a strong π interaction. In either case the results do not appear consistent with the results for $Fe(py)_4I_2$ and suggest that the I^- ions might not be in the first coordination sphere. These ambiguities could be resolved with knowledge of the crystal structure and the sign of the low temperature quadrupole splitting.

IV. Conclusion

The results of this work indicate that, in general, covalency effects in iron compounds have been greatly underestimated. In particular, treatments that assume that the Fe-H_2O bond is 100% ionic[1,4,23,24] are unjustified. The reduction of the spin orbit coupling constant from 148° to 40° or less reflects a great degree of ligand interaction. $Q.S._{lat}$ values calculated on the basis of a point charge model for Fe^{2+} six-fold coordinated with water are small (<.1 mm/sec).[14] Although a $Q.S._{lat}$ value has never been explicitly determined for $Fe(NH_4SO_4)_2 \cdot 6H_2O$ it seems highly unlikely that the $Q.S._{lig}$ value found for this compound (0.6 to 0.9 mm/sec) could be explained without allowing for some ligand to metal charge transfer. The differences in the $|Q.S._e|$ values for Fe coordinated with H_2O, 1,10 phenanthroline, pyridine, and CN^- indicate a substantial degree of d orbital-ligand interaction.

Since even Fe^{2+} high spin compounds cannot be treated satisfactorily with an ionic model several conclusions based on this model must be treated with skepticism. If the spin orbit coupling constant for the compound $Fe(NH_4SO_4)_2 \cdot 6H_2O$ is as small as we believe then the value for Q, the quadrupole moment for the Fe^{57} excited state, calculated on the basis of an ionic model[14] must be considerably underestimated. If the Fe^{2+} - H_2O bond cannot be considered as ionic then the Fe^{3+} - H_2O bond is surely covalent and the Mossbauer isomer shift model based on the ionicity of these compounds[24] is incorrect. In all likelihood Fe^{3+}

high spin compounds show smaller isomer shift values than Fe^{2+} high spin compounds simply because the 4s density is much greater in the more covalent Fe^{3+} compounds.[25]

Table I.

Compound	Temperature (°K)	Quadrupole Splitting (mm/sec)
$Fe(py)_4(SCN)_2$	294.2	1.538 ± .003
	261.7	1.625 ± .005
	227.7	1.730 ± .003
	196.7	1.829 ± .003
	140.2	1.987 ± .003
	120.2	2.011 ± .003
	98.7	2.033 ± .003
$Fe(py)_4I_2 \cdot 2py$	293.5	.548 ± .013
	248.2	.689 ± .008
	216.2	.775 ± .008
	187.4	.853 ± .006
	172.2	.901 ± .005
	149.2	.957 ± .004
	128.2	1.000 ± .004
	116.2	1.005 ± .003
	103.2	1.015 ± .003
$Fe(py)_4I_2$	295.0	.317 ± .007
	255.6	.337 ± .006
	228.5	.368 ± .006
	201.5	.388 ± .006
	171.5	.434 ± .005
	142.5	.462 ± .004
	126.1	.480 ± .004
	110.5	.498 ± .004
	99.4	.503 ± .004
$Fe(py)_4Cl_2$	294.0	3.144 ± .006
	248.2	3.275 ± .006
	225.2	3.323 ± .006
	197.4	3.392 ± .006
	172.8	3.430 ± .004
	150.8	3.458 ± .004
	149.4	3.460 ± .004

Table I. (Cont'd.)

Compound	Temperature (°K)	Quadrupole Splitting (mm/sec)
$Fe(NH_4SO_4)_2 \cdot 6H_2O$	295.0	1.721 ± .002
	246.9	1.968 ± .003
	204.2	2.185 ± .003
	167.4	2.368 ± .003
	162.2	2.418 ± .003
	137.1	2.519 ± .003
	114.8	2.618 ± .003
	102.2	2.673 ± .003
$K_3Fe(CN)_6$	294.2	.282 ± .003
	249.7	.308 ± .003
	200.5	.341 ± .004
	172.2	.359 ± .004
	149.2	.377 ± .003
	137.1	.385 ± .003
	125.0	.403 ± .003
	110.7	.428 ± .003
	99.7	.439 ± .003
$Fe(phen)_3(ClO_4)_3$	295.0	1.578 ± .003
	257.0	1.649 ± .005
	236.0	1.679 ± .003
	218.4	1.705 ± .004
	196.1	1.736 ± .004
	170.2	1.756 ± .003
	149.6	1.767 ± .003

Table II

	ground	1st level	not populated	Q.S.°	$Q.S._e$
	1. t_{2g}°	(t_{2g}^{+},t_{2g}^{-})	---	K $4/7\langle r^{-3}\rangle$	K-$4/7\langle r^{-3}\rangle$
Fe^{2+}	2. $(t_{2g}^{-},t_{2g}^{+}$	t_{2g}°	---	K-$2/7\langle r^{-3}\rangle$	K $2/7\langle r^{-3}\rangle$
high spin	3. t_{2g}°	$t_{2g}^{-}(t_{2g}^{+})$	$t_{2g}^{+}(t_{2g}^{-})$	K $4/7\langle r^{-3}\rangle$	K-$2/7\langle r^{-3}\rangle$
	4. $t_{2g}^{-}(t_{2g}^{+})$	t_{2g}°	$t_{2g}^{+}(t_{2g}^{-})$	K-$2/7\langle r^{-3}\rangle$	K $4/7\langle r^{-3}\rangle$

	ground	1st level	2nd level	Q.S.°	$Q.S._e$
Fe^{3+}	5. t_{2g}°	(t_{2g}^{-},t_{2g}^{+})	---	K $2/7\langle r^{-3}\rangle$	K-$2/7\langle r^{-3}\rangle$
low spin	6. (t_{2g}^{-},t_{2g}^{+})	t_{2g}°	---	K-$4/7\langle r^{-3}\rangle$	K+$4/7\langle r^{-3}\rangle$
		$\Delta E(t_{2g}^{-} \rightarrow t_{2g}^{\circ}) > \Delta E(t_{2g}^{\circ} \rightarrow t_{2g}^{+})$			
	7. $t_{2g}^{-}(t_{2g}^{+})$	t_{2g}°	$t_{2g}^{+}(t_{2g}^{-})$	K $2/7\langle r^{-3}\rangle$	K-$4/7\langle r^{-3}\rangle$

$$K = 1/2\ e^2Q$$

Table II. The values of Q.S.° and $Q.S._e$ expected for various orbital arrangements in the ionic case with no lattice effect. The cases where t_{2g}^{-} or t_{2g}^{+} might be degenerate with t_{2g}° are not included.

* This work was partially supported by the National Science Foundation, Grant GK871.

1. R. M. Sternheimer, Phys. Rev. 130, 1423 (1963)
2. A. J. Freeman and R. E. Watson, Phys. Rev. 131, 2566 (1963)
3. C. J. Ballhausen, Introduction to Ligand Field Theory (McGraw-Hill, New York, 1962)
4. M. Weissbluth, Structure and Bonding, 2, 1 (1967)
5. R. M. Golding, K. F. Mok and J. F. Duncan, Inorg. Chem. 5, 774 (1966)
6. N. E. Erickson, Ph.D. Thesis, University of Washington (1964)
7. J. Ullrich, Ph.D. Thesis, University of Michigan (1967)
8. W. T. Oosterhuis, G. Lang and S. de Bendetti, Phys. Letters 24A, 346 (1967)
9. E. Konig and A. S. Chakravarty, Theoret. Chim. Acta (Berl.) 9, 151 (1967)
10. R. E. Trees, Phys. Rev. 82, 683 (1951)
11. M. Eibschutz, U. Ganiel and S. Shtrikman, Phys. Rev. 156, 259 (1967)
12. R. Ingalls, Phys. Rev. 133, A787 (1964)
13. C. E. Johnson, W. Marshall, and G. E. Perlow, Phys. Rev. 126, 1503 (1962)
14. A. J. Nozik and M. Kaplan, Phys. Rev. 159, 273 (1967)
15. M. H. L. Pryce, Nuovo Cimento Suppl. 6, 817 (1957)
16. D. Palumbo, Nuovo Cimento 7, 271 (1958)
17. B. N. Figgis, Trans. Faraday Soc. 57, 198 (1961)

18. R. L. Collins and J. C. Travis, Mossbauer Effect Methodology 3, 123 (1967)

19. R. L. Collins, R. Pettit and W. A. Baker, J. Inorg. Nucl. Chem. 28, 1001 (1966)

20. R. M. Golding, Molecular Physics 12, 13 (1967)

21. P. B. Merrithew and P. G. Rasmussen (unpublished data)

22. I. Sotofte and S. E. Rasmussen, Acta Chem. Scand. 21, 2028 (1967)

23. L. Pauling, The Nature of the Chemical Bond (Cornell University Press, Ithaca, New York, 1960)

24. L. R. Walker, G. K. Wertheim, and V. Jaccarino, Phys. Rev. Letter 6, 98 (1961)

25. P. B. Merrithew (to be published)

Caption Page

Fig. 1. A typical spectrum. $Fe(py)_4(SCN)_2$ at 98.7°K. Velocity given vs $Na_2FeCN_5NO \cdot 2H_2O$ (NBS standard No. 725)

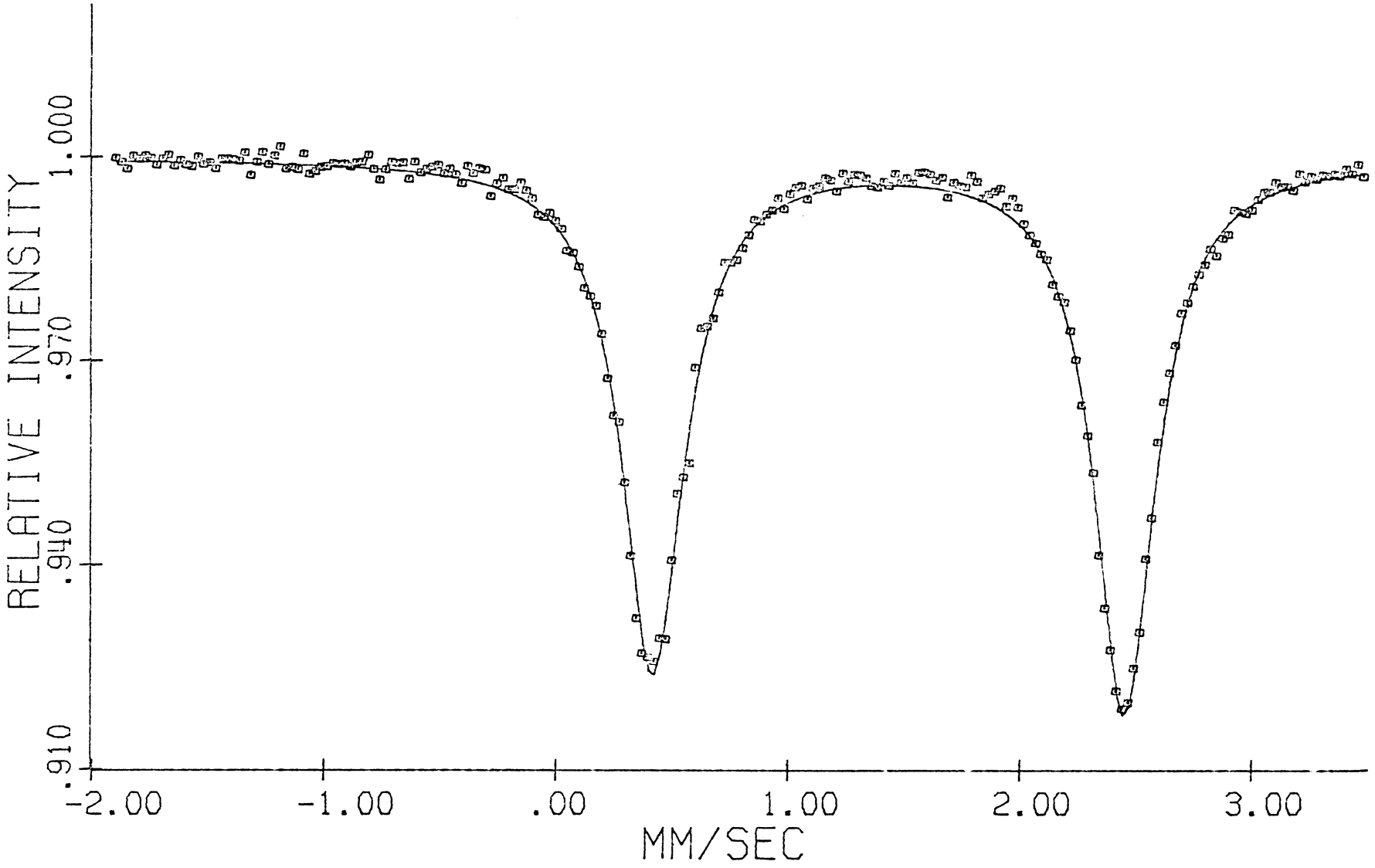
RELATIVE INTENSITY
1.000
.970
.940
.910
-2.00
-1.00
.00
1.00
2.00
3.00
MM/SEC

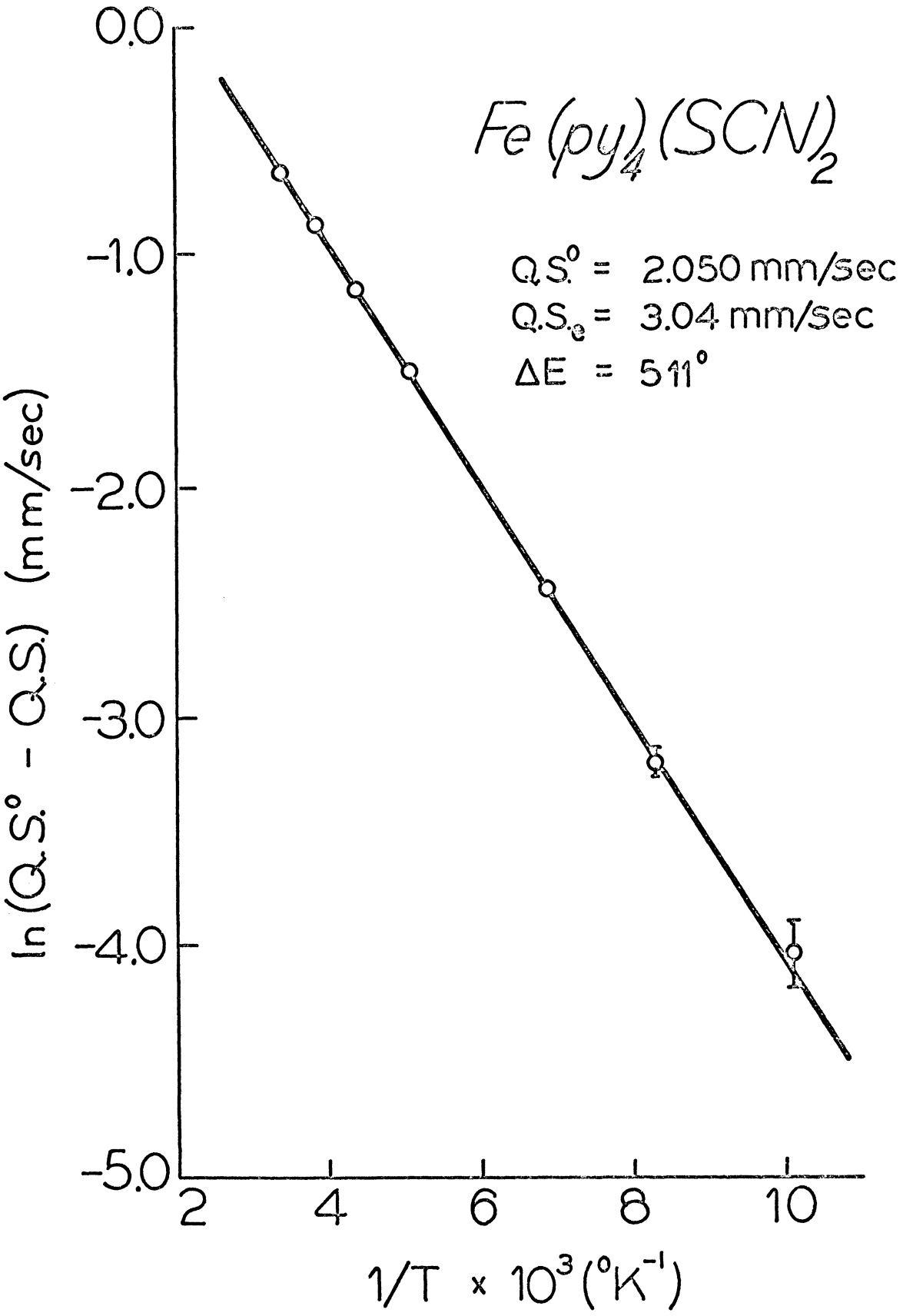
Fe(py)4(SCN)2
Q.S.° = 2.050 mm/sec
Q.S.e = 3.04 mm/sec
ΔE = 511°
0.0
-1.0
-2.0
-3.0
-4.0
-5.0
ln(Q.S.° - Q.S.) (mm/sec)
2
4
6
8
10
1/T × 10³ (°K⁻¹)

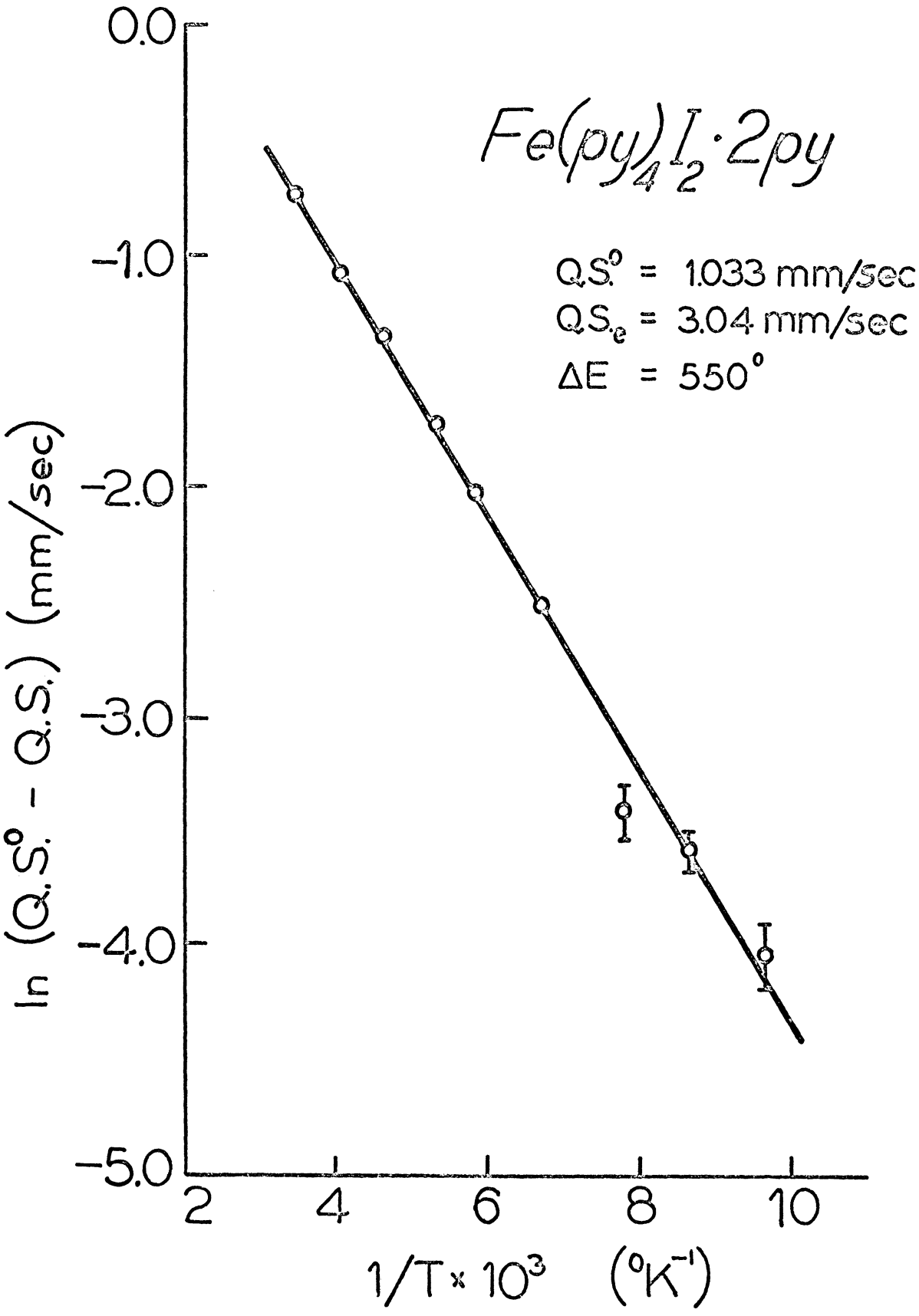
$Fe(py)_4I_2 \cdot 2py$
$Q.S.^{\circ}$ = 1.033 mm/sec
$Q.S._e$ = 3.04 mm/sec
ΔE = 550°
0.0
-1.0
-2.0
-3.0
-4.0
-5.0
ln (Q.S.° - Q.S.) (mm/sec)
2
4
6
8
10
1/T × 10³ (°K⁻¹)

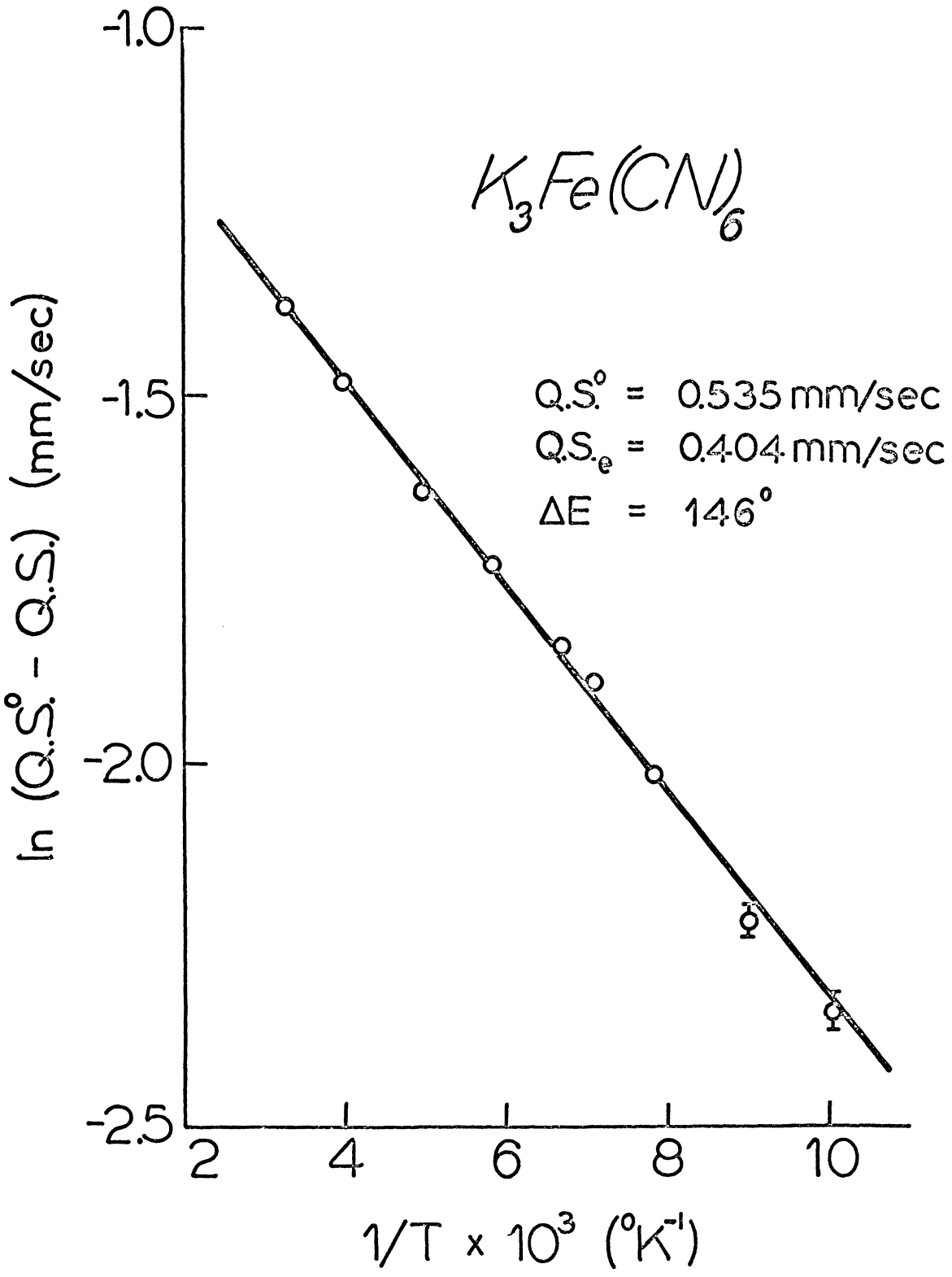
$K_3Fe(CN)_6$
Q.S.° = 0.535 mm/sec
$Q.S._e$ = 0.404 mm/sec
ΔE = 146°
ln (Q.S.° - Q.S.) (mm/sec)
-1.0
-1.5
-2.0
-2.5
2
4
6
8
10
1/T x 10^3 (°K^{-1})

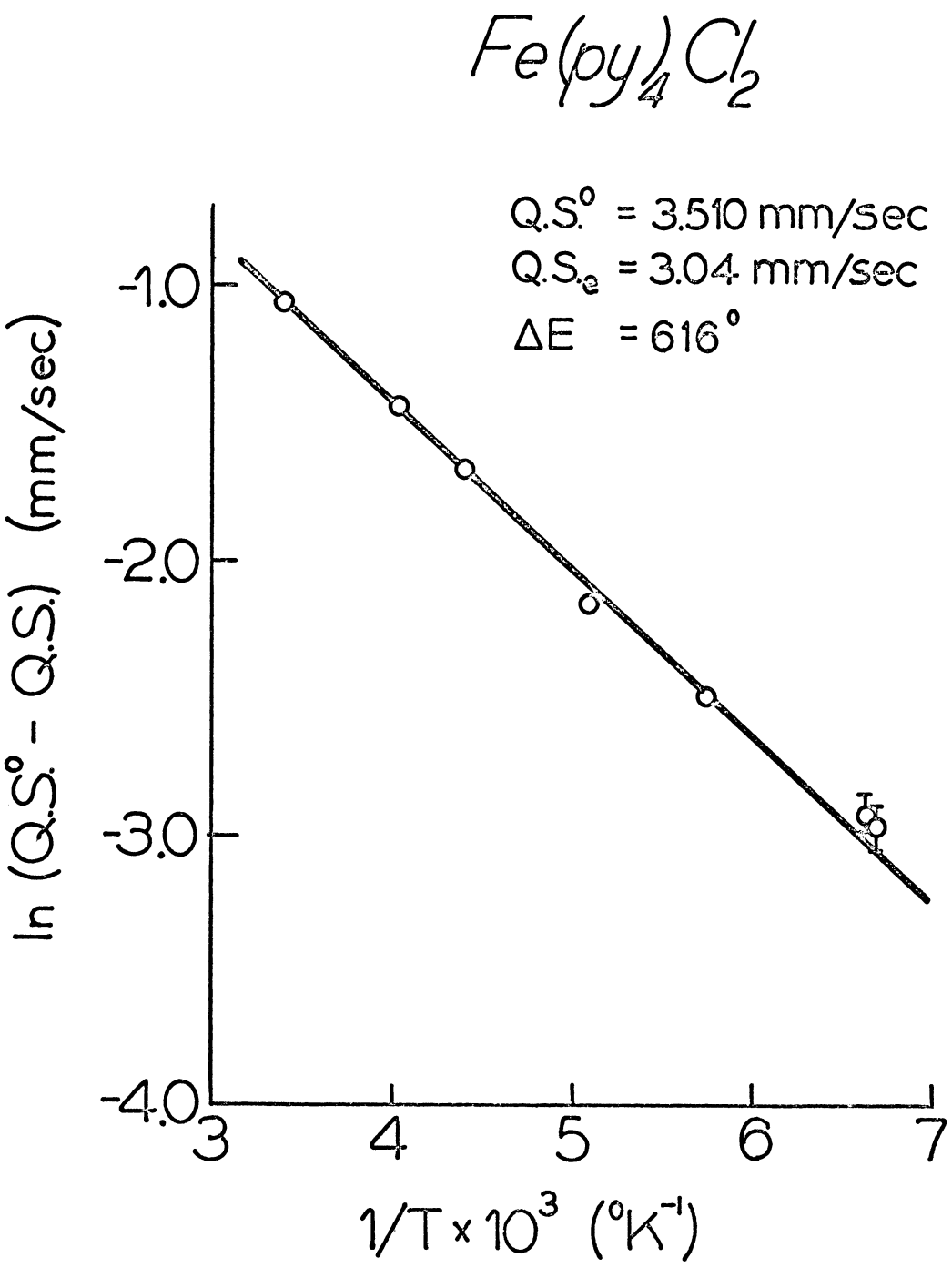
Fe(py)4Cl2
Q.S.° = 3.510 mm/sec
Q.Se = 3.04 mm/sec
ΔE = 616°
ln (Q.S.° - Q.S.) (mm/sec)
-1.0
-2.0
-3.0
-4.0
3
4
5
6
7
1/T x 10³ (°K⁻¹)

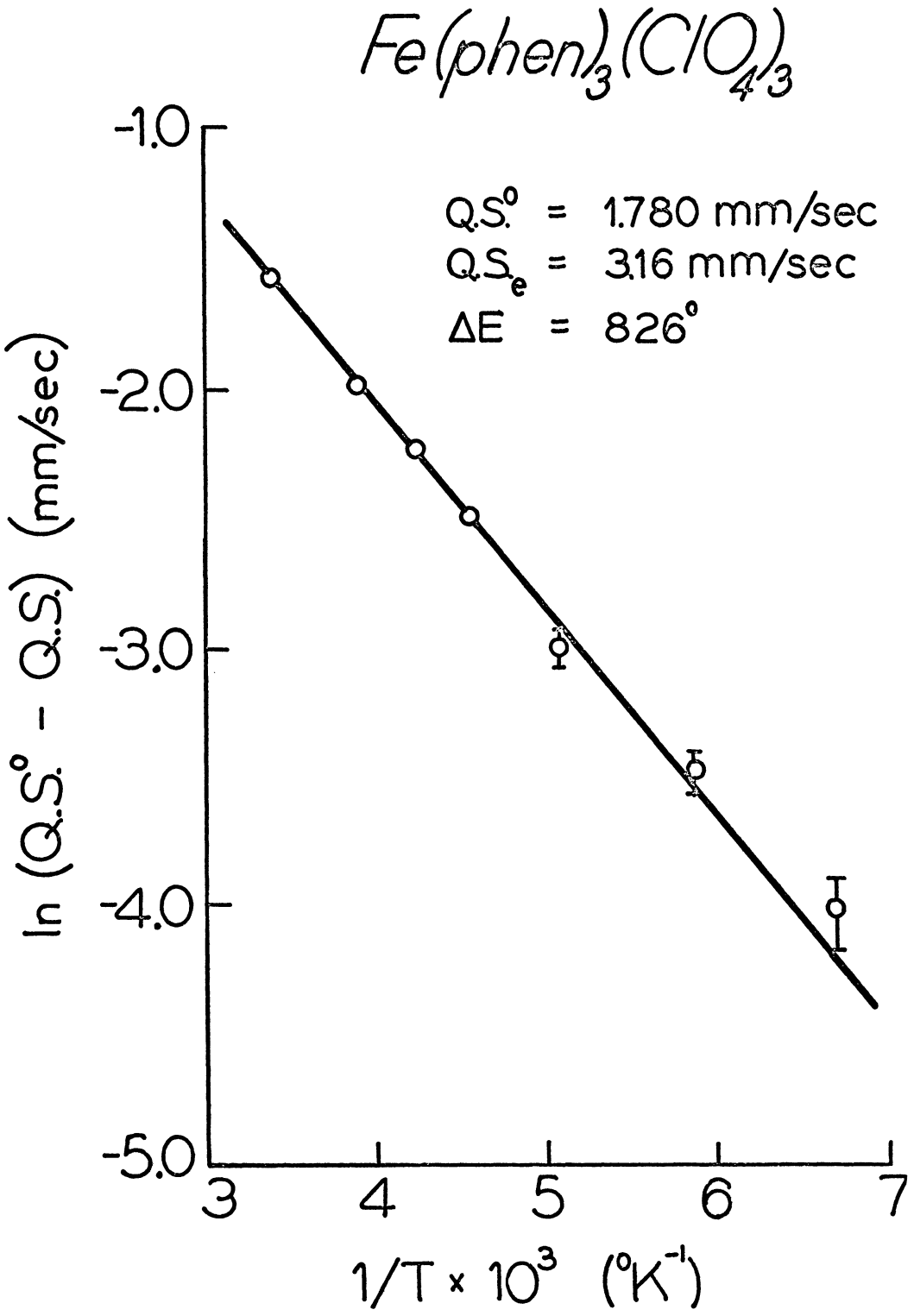
Fe(phen)3(ClO4)3
Q.S.° = 1.780 mm/sec
Qe = 3.16 mm/sec
ΔE = 826°
ln (Q.S.° - Q.S.) (mm/sec)
-1.0
-2.0
-3.0
-4.0
-5.0
3
4
5
6
7
1/T × 10³ (°K⁻¹)

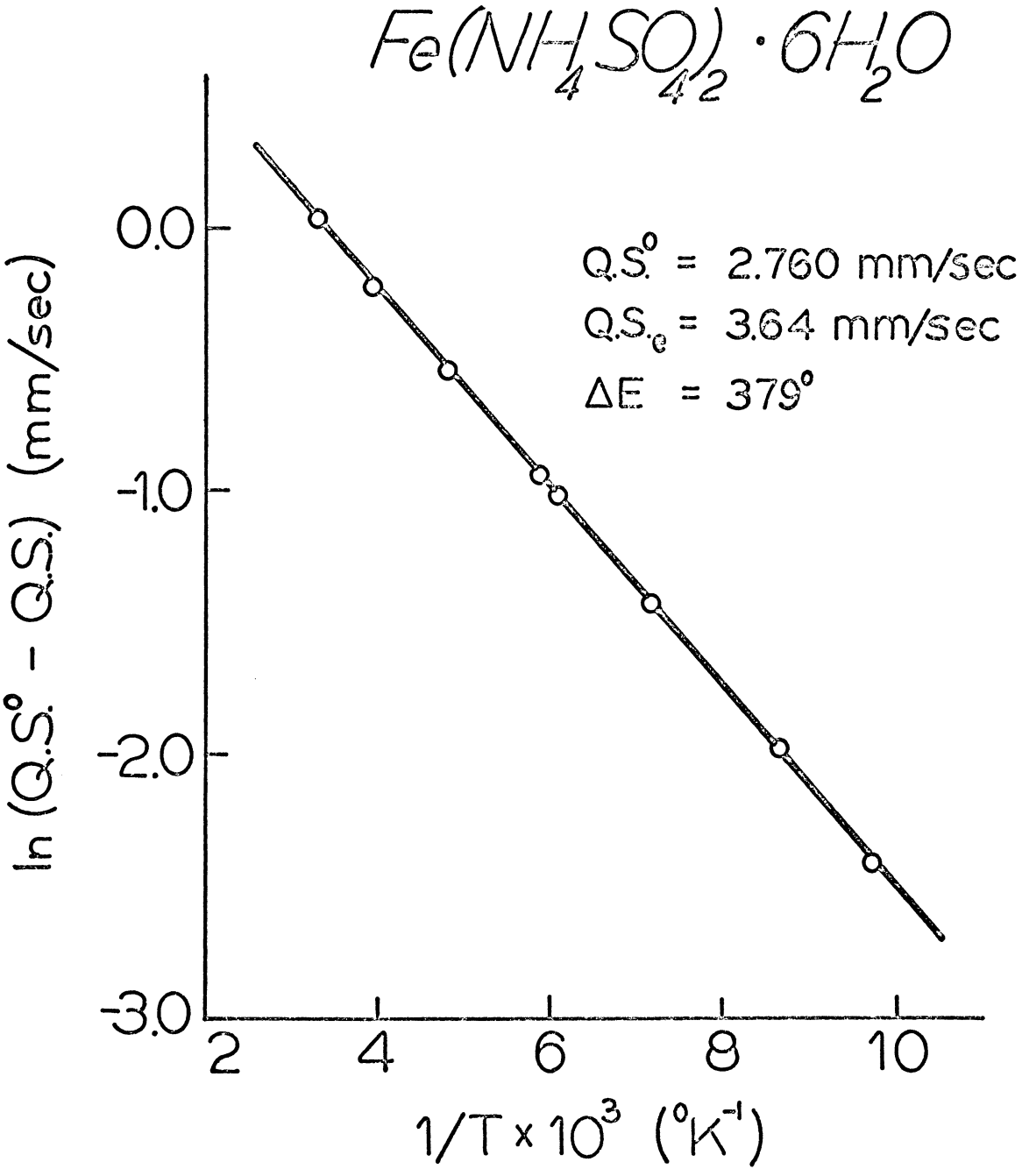
$Fe(NH_4SO_4)_2 \cdot 6H_2O$
Q.S.° = 2.760 mm/sec
Q.S.$_e$ = 3.64 mm/sec
ΔE = 379°
0.0
-1.0
-2.0
-3.0
2
4
6
8
10
ln (Q.S.° - Q.S.) (mm/sec)
1/T x 10^3 (°K^{-1})

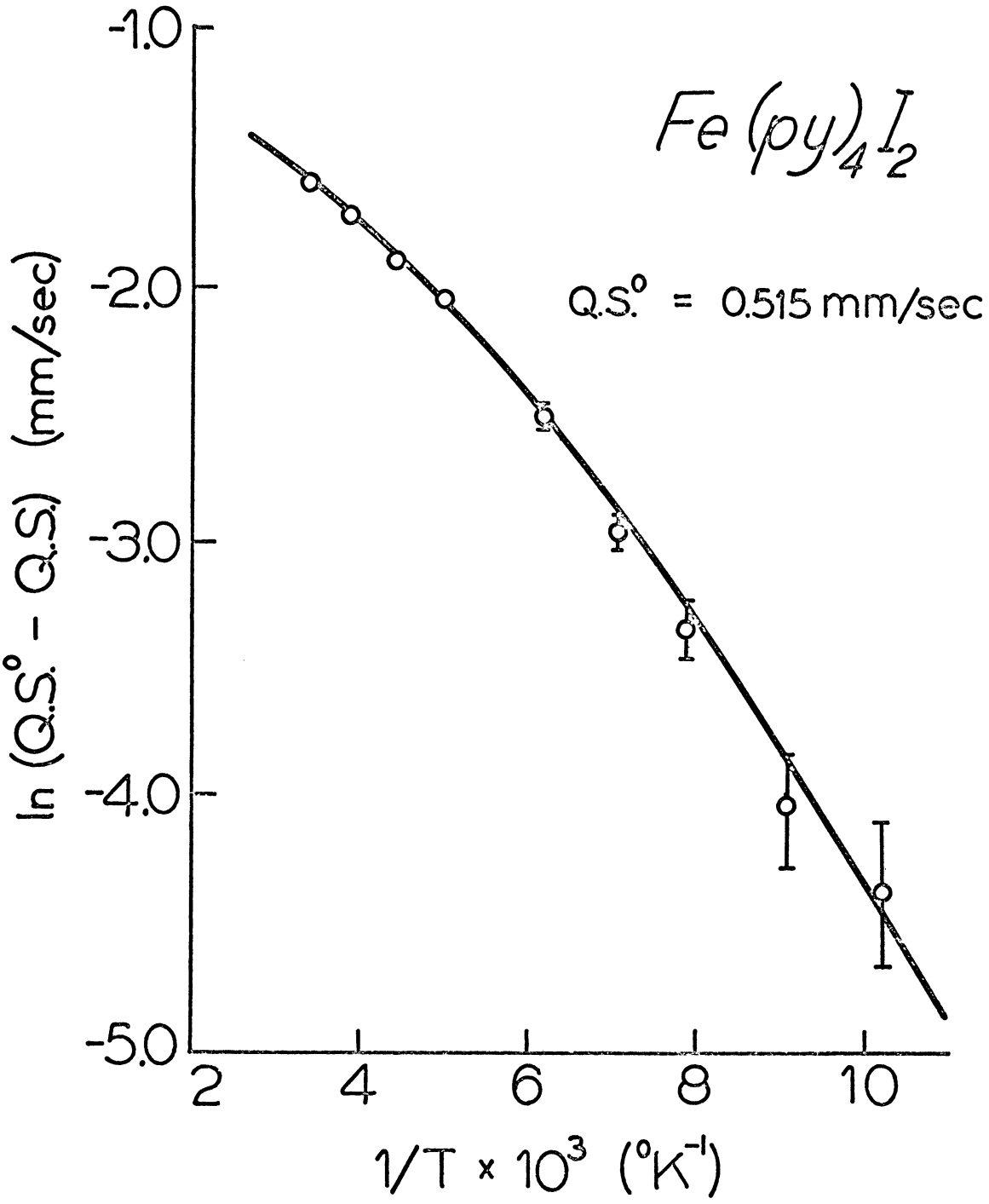
Fe(py)4I2
Q.S.° = 0.515 mm/sec
ln (Q.S.° - Q.S.) (mm/sec)
-1.0
-2.0
-3.0
-4.0
-5.0
2
4
6
8
10
1/T x 10³ (°K⁻¹)